J|A|C|S ARTICLES

Published on Web 07/29/2009

Highly Selective Biaryl Cross-Coupling Reactions between Aryl Halides and Aryl Grignard Reagents: A New Catalyst Combination of *N*-Heterocyclic Carbenes and Iron, Cobalt, and Nickel Fluorides

Takuji Hatakeyama,[†] Sigma Hashimoto,[†,‡] Kentaro Ishizuka,[†,§] and Masaharu Nakamura*[,†,§]

International Research Center for Elements Science, Institute for Chemical Research, Department of Energy and Hydrocarbon Chemistry, Graduate School of Engineering, and Institute of Sustainability Science, Kyoto University, Uji, Kyoto 611-0011, Japan

Received May 14, 2009; E-mail: masaharu@scl.kyoto-u.ac.jp

Abstract: Combinations of *N*-heterocyclic carbenes (NHCs) and fluoride salts of the iron-group metals (Fe, Co, and Ni) have been shown to be excellent catalysts for the cross-coupling reactions of aryl Grignard reagents (Ar^1MgBr) with aryl and heteroaryl halides (Ar^2X) to give unsymmetrical biaryls (Ar^1-Ar^2). Iron fluorides in combination with SIPr, a saturated NHC ligand, catalyze the biaryl cross-coupling between various aryl chlorides and aryl Grignard reagents in high yield and high selectivity. On the other hand, cobalt and nickel fluorides in combination with IPr, an unsaturated NHC ligand, exhibit interesting complementary reactivity in the coupling of aryl bromides or iodides; in contrast, with these substrates the iron catalysts show a lower selectivity. The formation of homocoupling byproducts is suppressed markedly to less than 5% in most cases by choosing the appropriate metal fluoride/NHC combination. The present catalyst combinations offer several synthetic advantages over existing methods: practical synthesis of a broad range of unsymmetrical biaryls without the use of palladium catalysts and phosphine ligands. On the basis of stoichiometric control experiments and theoretical studies, the origin of the unique catalytic effect of the fluoride counterion can be ascribed to the formation of a higher-valent heteroleptic metalate $[Ar^1MF_2]MgBr$ as the key intermediate in our proposed catalytic cycle. First, stoichiometric control experiments revealed the stark differences in chemical reactivity between the metal fluorides and metal chlorides. Second, DFT calculations indicate that the initial reduction of di- or trivalent metal fluoride in the wake of transmetalation with PhMgCl is energetically unfavorable and that formation of a divalent heteroleptic metalate complex, $[PhMF_2]MgCl$ (M = Fe, Co, Ni), is dominant in the metal fluoride system. The heteroleptic ate-complex serves as a key reactive intermediate, which undergoes oxidative addition with PhCl and releases the biaryl cross-coupling product Ph−Ph with reasonable energy barriers. The present cross-coupling reaction catalyzed by iron-group metal fluorides and an NHC ligand provides a highly selective and practical method for the synthesis of unsymmetrical biaryls as well as the opportunity to gain new mechanistic insights into the metal-catalyzed cross-coupling reactions.

Introduction

Biaryls are important structural units for a wide range of functional molecules,[1] such as chiral ligands and catalysts, drug intermediates, liquid crystals, physiologically active natural products, organic electronic materials, and functional polymers. Because of the significance and prevalence of this class of compounds, numerous synthetic methods have been developed for over a century.[2] Reductive homocoupling of aryl halides or pseudohalides i.e., the classical Ullmann reaction, has been developed to give the desired symmetrical biaryls using various transition metals,[2a,c] palladium catalysts in combination with appropriate terminal reductants such as zinc are currently the prevailing choice.[2b] Furthermore, the cross-coupling of two different aryl halides under reducing conditions has been also developed.[3] The oxidative counterpart of the biaryl synthesis has also enhanced its utility

[†] International Research Center for Elements Science (IRCELS), Institute for Chemical Research, Kyoto University.
[‡] Department of Energy and Hydrocarbon Chemistry, Kyoto University.
[§] Institute of Sustainability Science, Kyoto University.

(1) (a) Demus, D., Goodby, J. W., Gray, G. W., Spiess, H.-W., Vill, V., Eds. *Handbook of Liquid Crystals*; Wiley-VCH: Weinheim, 1998. (b) Mitschke, U.; Bauerle, P. *J. Mater. Chem.* **2000**, *10*, 1471–1507. (c) Yamamoto, T. *J. Organomet. Chem.* **2002**, *653*, 195–199. (d) Baudoin, O.; Gueritte, F. *Stud. Nat. Prod. Chem., Part J* **2003**, *29*, 355–417. (e) Holder, E.; Langeveld, B. M. W.; Schubert, U. S. *Adv. Mater.* **2005**, *17*, 1109–1121. (f) Ambade, A. V.; Savariar, E. N.; Thayumanavan, S. *Mol. Pharm.* **2005**, *2*, 264–272. (g) Doucet, H.; Hierso, J.-C. *Curr. Opin. Drug Discovery Devel.* **2007**, *10*, 672–690. (h) Abe, H.; Harayama, T. *Heterocycles* **2008**, *75*, 1305–1320.

(2) (a) Cepanec, I., Ed. *Synthesis of Biaryls*; Elsevier Ltd: Oxford, 2004. (b) Hassan, J.; Sévignon, M.; Gozzi, C.; Schulz, E.; Lemaire, M. *Chem. Rev.* **2002**, *102*, 1359–1469. (c) Nelson, T. D.; Crouch, R. D. *Org. React.* **2004**, *63*, 265–555. (d) Corbet, J. P.; Mignani, G. *Chem. Rev.* **2006**, *106*, 2651–2710.

(3) Amatore, M.; Gosmini, C. *Angew. Chem., Int. Ed.* **2008**, *47*, 2089–2092, and references cited therein.

 © 2009 American Chemical Society

since the seminal work of Kharasch and co-workers who discovered that aryl Grignard reagents undergo efficient homocoupling in the presence of catalytic amounts of first-row transition metal salts, such as the chloride salts of chromium, manganese, iron, cobalt, nickel, and copper.[4] Indeed, recent progress in this oxidative coupling chemistry has extended their utility to the synthesis of various functionalized biaryls.[5] The advancement of both reductive and oxidative biaryl coupling reactions notwithstanding, transition metal-catalyzed cross-coupling reactions are the popular choice, holding the synthetic advantages such as high selectivity, broad substrate scopes, and mild reaction conditions.[6] In fact, a wide range of arylmetal compounds has been successfully utilized to date as the nucleophilic partner in unsymmetrical biaryl coupling reactions (Scheme 1). While one may use aryllithium,[7] magnesium,[8] boron,[9] silicon,[10] copper,[11] zinc,[12] or tin compounds,[13] arylmagnesium compounds seem ideal for practical synthesis because they are

Scheme 1. Transition Metal-Catalyzed Biaryl Coupling Reaction

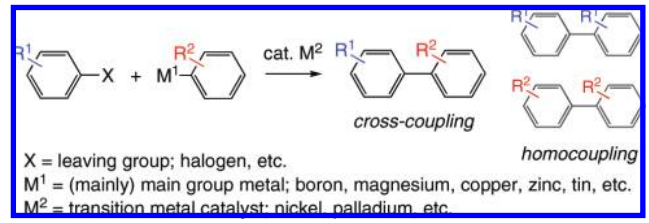

readily available, cheap and environmentally benign. Despite these synthetic advantages of arylmagnesium compounds, there is one serious drawback associated with their use: the considerable generation of the symmetrical biaryls via undesired homocouplings of the arylmagnesium compound and/or the aryl electrophile. This issue often hampers their general application for industrial production of biaryls.

We have been interested in the development of iron-catalyzed reactions,[14−16] and launched a thorough investigation of iron catalysis to overcome the above-mentioned synthetic problem associated with the unwanted homocou-

(4) Kharasch, M. S.; Fields, E. K. *J. Am. Chem. Soc.* **1941**, *63*, 2316–2320.

(5) Recent papers: (a) Nagano, T.; Hayashi, T. *Org. Lett.* **2005**, *7*, 491–493. (b) Cahiez, G.; Chaboche, C.; Mahuteau-Betzer, F.; Ahr, M. *Org. Lett.* **2005**, *7*, 1943–1946. (c) Cahiez, G.; Moyeux, A.; Buendia, J.; Duplais, C. *J. Am. Chem. Soc.* **2007**, *129*, 13788–13789. Without metal catalysts. (d) Krasovskiy, A.; Tishkov, A.; del Amo, V.; Mayr, H.; Knochel, P. *Angew. Chem., Int. Ed.* **2006**, *45*, 5010–5014.

(6) (a) de Meijere, A., Diederich, F., Eds. *Metal-Catalyzed Cross-coupling Reactions*, 2nd ed.; Wiley-VCH: Germany, 2004. (b) Miyaura, N., Ed.; *Cross-Coupling Reactions: A Practical Guide*; Springer: Berlin, 2002. (c) Stanforth, S. P. *Tetrahedron* **1998**, *54*, 263–303.

(7) (a) Snieckus, V. *Chem. Rev.* **1990**, *90*, 879–933. (b) Murahashi, S. *J. Organomet. Chem.* **2002**, *653*, 27–33. (c) Anctil, E. J.-G.; Snieckus, V. *J. Organomet. Chem.* **2002**, *653*, 150–160. (d) Nájera, C.; Sansano, J. M.; Yus, M. *Tetrahedron* **2003**, *59*, 9255–9303.

(8) (a) Tamao, K. *J. Organomet. Chem.* **2002**, *653*, 23–26. (b) Banno, T.; Hayakawa, Y.; Umeno, M. *J. Organomet. Chem.* **2002**, *653*, 288–291. (c) Knochel, P.; Dohle, W.; Gommermann, N.; Kneisel, F. F.; Kopp, F.; Korn, T.; Sapountzis, I.; Vu, V. A. *Angew. Chem., Int. Ed.* **2003**, *42*, 4302–4320. (d) Ila, H.; Baron, O.; Wagner, A. J.; Knochel, P. *Chem. Lett.* **2006**, *35*, 2–7. (e) Terao, J.; Kambe, N. *Acc. Chem. Res.* **2008**, *41*, 1545–1554.

(9) (a) Miyaura, N.; Suzuki, A. *Chem. Rev.* **1995**, *95*, 2457–2483. (b) Lloyd-Williams, P.; Giralt, E. *Chem. Soc. Rev.* **2001**, *30*, 145–157. (c) Miyaura, N. *J. Organomet. Chem.* **2002**, *653*, 54–57. (d) Suzuki, A. *J. Organomet. Chem.* **2002**, *653*, 83–90. (e) Miyaura, N. *Top. Curr. Chem.* **2002**, *219*, 11–59. (f) Kotha, S.; Lahiri, K.; Kashinath, D. *Tetrahedron* **2002**, *58*, 9633–9695. (g) Bellina, F.; Carpita, A.; Rossi, R. *Synthesis* **2004**, 2419–2440. (h) Ishiyama, T.; Miyaura, N. *Pure Appl. Chem.* **2006**, *78*, 1369–1375. (i) Molander, G. A.; Ellis, N. *Acc. Chem. Res.* **2007**, *40*, 275–286. (j) Darses, S.; Genet, J.-P. *Chem. Rev.* **2008**, *108*, 288–325. (k) Doucet, H. *Eur. J. Org. Chem.* **2008**, 2013–2030.

(10) (a) Hiyama, T.; Hatanaka, Y. *Pure Appl. Chem.* **1994**, *66*, 1471–1478. (b) Hiyama, T.; Shirakawa, E. *Top. Curr. Chem.* **2002**, *219*, 61–85. (c) Denmark, S. E.; Sweis, R. F. *Acc. Chem. Res.* **2002**, *35*, 835–846. (d) Hiyama, T. *J. Organomet. Chem.* **2002**, *653*, 58–61. (e) Denmark, S. E.; Pan, W. *J. Organomet. Chem.* **2002**, *653*, 98–104. (f) Denmark, S. E.; Ober, M. H. *Aldrichimica Acta* **2003**, *36*, 75–85. (g) Spivey, A. C.; Gripton, C. J. G.; Hannah, J. P. *Curr. Org. Synth.* **2004**, *1*, 211–226. (h) Denmark, S. E.; Baird, J. D. *Chem.−Eur. J.* **2006**, *12*, 4954–4963. (i) Denmark, S. E.; Regens, C. S. *Acc. Chem. Res.* **2008**, *41*, 1486–1499.

(11) (a) Taylor, R. J. K. Ed.; *Organocopper Reagents*; Oxford University Press: Oxford, 1994. (b) Lipshutz, B. H. *Acc. Chem. Res.* **1997**, *30*, 277–282. (c) Krause, N.; Gerold, A. *Angew. Chem., Int. Ed.* **1997**, *36*, 187–204. (d) Woodward, S. *Chem. Soc. Rev.* **2000**, *29*, 393–401. (e) Krause, N. Ed.; *Modern Organocopper Chemistry*, Wiley-VCH, Weinheim, 2002. (f) Nakamura, E.; Mori, S. *Angew. Chem., Int. Ed.* **2000**, *39*, 3751–3771. (g) Caprio, V. *Lett. Org. Chem.* **2006**, *3*, 339–349.

(12) (a) Negishi, E. *Acc. Chem. Res.* **1982**, *15*, 340–348. (b) Knochel, P., Jones, P., Eds. *Organozinc Reagents*; Oxford University Press: Oxford, 1999. (c) Negishi, E. *J. Organomet. Chem.* **2002**, *653*, 34–40. (d) Lessene, G. *Aust. J. Chem.* **2004**, *57*, 107. (e) Zvi, R., Marek, I. Eds. *Chemistry of Organozinc Compounds*; John Wiley: Chichester, 2006.

(13) (a) Stille, J. K. *Angew. Chem., Int. Ed. Engl.* **1986**, *25*, 508–523. (b) Mitchell, T. N. *J. Organomet. Chem.* **1986**, *304*, 1–16. (c) Mitchell, T. N. *Synthesis* **1992**, 803–815. (d) Kosugi, M.; Fugami, K. *J. Organomet. Chem.* **2002**, *653*, 50–53. (e) Espinet, P.; Echavarren, A. M. *Angew. Chem., Int. Ed.* **2004**, *43*, 4704–4734. (f) Echavarren, A. M. *Angew. Chem., Int. Ed.* **2005**, *44*, 3962–3965.

(14) Reviews: (a) Plietker, B. Ed. *Iron Catalysis in Organic Chemistry*; Wiley-VCH: Weinheim, 2008. (b) Bolm, C.; Legros, J.; Le Paih, J.; Zani, L. *Chem. Rev.* **2004**, *104*, 6217–6254. (c) Shinokubo, H.; Oshima, K. *Eur. J. Org. Chem.* **2004**, 2081–2091. (d) Fürstner, A.; Martin, R. *Chem. Lett.* **2005**, *34*, 624–629. (e) Correa, A.; Mancheño, O. G.; Bolm, C. *Chem. Soc. Rev.* **2008**, *37*, 1108–1117. (f) Sherry, B. D.; Fürstner, A. *Acc. Chem. Res.* **2008**, *41*, 1500–1511.

(15) Iron-catalyzed cross-coupling reactions of sp2-carbon electrophiles: (a) Tamura, M.; Kochi, J. K. *J. Am. Chem. Soc.* **1971**, *93*, 1487–1489. (b) Fabre, J.-L.; Julia, M.; Verpeaux, J.-N. *Tetrahedron Lett.* **1982**, *23*, 2469–2472. (c) Molander, G. A.; Rahn, B. J.; Shubert, D. C.; Bonde, S. E. *Tetrahedron Lett.* **1983**, *24*, 5449–5452. (d) Reddy, C. K.; Knochel, P. *Angew. Chem., Int. Ed. Engl.* **1996**, *35*, 1700–1701. (e) Cahiez, G.; Avedissian, H. *Synthesis* **1998**, 1199–1205. (f) Fürstner, A.; Leitner, A.; Méndez, M.; Krause, H. *J. Am. Chem. Soc.* **2002**, *124*, 13856–13863. (g) Necas, D.; Kotora, M.; Císarová, I. *Eur. J. Org. Chem.* **2004**, 1280–1285. (h) Duplais, C.; Bures, F.; Sapountzis, I.; Korn, T. J.; Cahiez, G.; Knochel, P. *Angew. Chem., Int. Ed.* **2004**, *43*, 2968–2970. (i) Itami, K.; Higashi, S.; Mineno, M.; Yoshida, J. *Org. Lett.* **2005**, *7*, 1219–1222. (j) Dunet, G.; Knochel, P. *Synlett* **2006**, 407–410. (k) Cahiez, G.; Gager, O.; Habiak, V. *Synthesis* **2008**, 2636–2644. (l) Cahiez, G.; Habiak, V.; Gager, O. *Org. Lett.* **2008**, *10*, 2389–2392. (m) Carril, M.; Correa, A.; Bolm, C. *Angew. Chem., Int. Ed.* **2008**, *47*, 4862–4865. (n) Hatakeyama, T.; Yoshimoto, Y.; Gabriel, T.; Nakamura, M. *Org. Lett.* **2008**, *10*, 5341–5344. (o) Fürstner, A.; Martin, R.; Krause, H.; Seidel, G.; Goddard, R.; Lehmann, C. W. *J. Am. Chem. Soc.* **2008**, *130*, 8773–8787.

(16) Iron-catalyzed cross-coupling reactions of sp3-carbon electrophiles: (a) Nakamura, M.; Matsuo, K.; Ito, S.; Nakamura, E. *J. Am. Chem. Soc.* **2004**, *126*, 3686–3687. (b) Nagano, T.; Hayashi, T. *Org. Lett.* **2004**, *6*, 1297–1299. (c) Martin, R.; Fürstner, A. *Angew. Chem., Int. Ed.* **2004**, *43*, 3955–3957. (d) Bedford, R. B.; Bruce, D. W.; Frost, R. M.; Goodby, J. W.; Hird, M. *Chem. Commun.* **2004**, 2822–2823. (e) Nakamura, M.; Ito, S.; Matsuo, K.; Nakamura, E. *Synlett* **2005**, 1794–1798. (f) Bedford, R. B.; Betham, M.; Bruce, D. W.; Danopoulos, A. A.; Frost, R. M.; Hird, M. *J. Org. Chem.* **2006**, *71*, 1104–1110. (g) Plietker, B. *Angew. Chem., Int. Ed.* **2006**, *45*, 1469–1473. (h) Dongol, K. G.; Koh, H.; Sau, M.; Chai, C. L. L. *Adv. Synth. Catal.* **2007**, *349*, 1015–1018. (i) Cahiez, G.; Habiak, V.; Duplais, C.; Moyeux, A. *Angew. Chem., Int. Ed.* **2007**, *46*, 4364–4366. (j) Cahiez, G.; Duplais, C.; Moyeux, A. *Org. Lett.* **2007**, *9*, 3253–3254. (k) Guérinot, A.; Reymond, S.; Cossy, J. *Angew. Chem., Int. Ed.* **2007**, *46*, 6521–6524. (l) Rao Volla, C.-M.; Vogel, P. *Angew. Chem., Int. Ed.* **2008**, *47*, 1305–1307. (m) Bedford, R. B.; Huwe, M.; Wilkinson, M. C. *Chem. Commun.* **2009**, 600–602. (n) Hatakeyama, T.; Kondo, Y.; Fujiwara, Y.; Takaya, H.; Ito, S.; Nakamura, E.; Nakamura, M. *Chem. Commun.* **2009**, 1216–1218.

Scheme 2. Selective Biaryl Cross-Coupling with an Iron Fluoride Catalyst

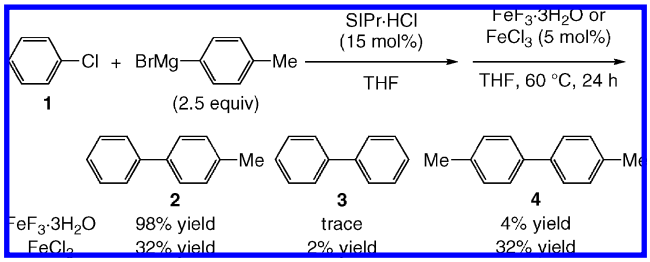

pling. We recently reported that the combination of iron fluoride and *N*-heterocyclic carbene (NHC) ligand is a highly selective and practical catalyst for biaryl cross-coupling reaction of arylmagnesium compounds (Scheme 2).[17] Metal fluorides have been known to show unique reactivity and selectivity in transition metal-catalyzed carbon−carbon bond-forming reactions such as the asymmetric Mukaiyama−Aldol reaction (copper),[18] allylation reaction (titanium),[19] as well as carbon−heteroatom bond-forming reactions, hydroamination reaction (iridium),[20] and hydrosilylation reaction (titanium).[21] While such a "fluoride effect" has attracted considerable interests in synthetic chemistry[22] as well as inorganic/organometallic chemistry, it remains unstudied in the field of transition metal-catalyzed cross-coupling reactions.[23,24] We have continued careful investigation on the "fluoride effect" in cobalt-[25] and nickel-catalyzed[26] cross-coupling reactions to achieve markedly selective biaryl cross-coupling of aryl halides with arylmagnesium compounds, and herein, report on the full details of this synthetically useful unsymmetrical biaryl synthesis with new catalyst combinations consisting of NHC ligand and the iron-group metal fluorides.

Results and Discussion

Iron Fluoride/NHC-Catalyzed Biaryl Cross-Coupling Reaction. We began our investigation focusing on the iron-catalysts because no general and practical method had theretofore been developed for iron-catalyzed biaryl cross-coupling reactions.[14−17] Whereas efficient homocoupling reactions of arylmagnesium compounds have been achieved using iron catalysts,[5a,b,d] only a few reports were reported for the iron-catalyzed cross-coupling reactions before our study[27] and a few more[28] in the last two years. We thus conducted a careful and detailed catalyst screening for the reaction of a simple aryl chloride with an arylmagnesium reagent. The benchmark coupling reaction was performed by heating a THF solution of chlorobenzene **1**, *p*-tolylmagnesium bromide (*p*-TolMgBr, 2.5 equiv), an iron salt (5 mol %), and an additive at 60 °C for 24 h (Table 1). Various additives, including imidazolium and imidazolinium salts (as shown in Chart 1), as well as typical phosphine ligands, were studied in combination with a catalytic amount of iron fluorides.

The optimum yield (98%) of 4-methylbiphenyl **2** was achieved with 5 mol % of $FeF_3 \cdot 3H_2O$ and 15 mol % of SIPr·HCl (entry 1). The undesired homocoupling reaction occurred only sluggishly and gave a negligible amount of biphenyl **3** and a small amount of 4,4′-dimethylbiphenyl **4** (0.018 mmol, 4% yield, based on the amount of *p*-TolMgBr). As shown in entry 2, when the less sterically demanding NHC was used, a lower conversion of the starting chlorobenzene **1** was observed. The unsaturated NHC precursors, IPr·HCl and I-*t*-Bu·HCl, were ineffective (entries 3 and 5). The counteranion of the NHC precursors has a considerable effect on the reactivity (entry 4). The use of 10 or 5 mol % of SIPr·HCl resulted in a selective, but slower, conversion (entries 6 and 7). The reaction was sluggish without an NHC precursor (entry 8). Tricyclohexylphosphine (PCy_3) did not accelerate the reaction (entry 9). As shown in entries 10−13, bidentate phosphine ligands and nitrogen ligands were found to inhibit the reaction.

Entries 14−21 show a striking contrast in the reactivity of various iron salts. Iron(II) fluoride tetrahydrate ($FeF_2 \cdot 4H_2O$) showed a comparable catalytic activity to afford **2** in 96% yield. The reaction did not complete with anhydrous FeF_3 or FeF_2, probably due to their lower solubility in THF (entries 15 and

(17) Hatakeyama, T.; Nakamura, M. *J. Am. Chem. Soc.* **2007**, *129*, 9844–9845.
(18) Krüger, J.; Carreira, E. M. *J. Am. Chem. Soc.* **1998**, *120*, 837–838.
(19) Gauthier, D. R.; Carreira, E. M. *Angew. Chem., Int. Ed.* **1996**, *35*, 2363–2365.
(20) Dorta, R.; Egli, P.; Zürcher, F.; Togni, A. *J. Am. Chem. Soc.* **1997**, *119*, 10857–10858.
(21) Verdaguer, X.; Lange, U. E. W.; Reding, M. T.; Buchwald, S. L. *J. Am. Chem. Soc.* **1996**, *118*, 6784–6785.
(22) Reviews: (a) Pagenkopf, B. L.; Carreira, E. M. *Chem. Eur. J.* **1999**, *5*, 3437–3442. (b) Fagnou, K.; Lautens, M. *Angew. Chem., Int. Ed.* **2002**, *41*, 26–47.
(23) Concomitant halide effect on palladium- or nickel-catalyzed cross-coupling and Heck reactions has been investigated for chloride, bromide, and iodide ions but not for fluoride ions: Amatore, C.; Jutand, A. *Acc. Chem. Res.* **2000**, *33*, 314–321, and references cited therein.
(24) Activation of organometal compounds with a stoichiometric amount of fluoride ion in cross-coupling reactions. Boron: (a) Wright, S. W.; Hageman, D. L.; McClure, L. D. *J. Org. Chem.* **1994**, *59*, 6095–6097. (b) Darses, S.; Michaud, G.; Genet, J.-P. *Eur. J. Org. Chem.* **1999**, 1875–1883. (c) Molander, G. A.; Biolatto, B. *J. Org. Chem.* **2003**, *68*, 4302–4314. Silane: (d) Hatanaka, Y.; Hiyama, T. *J. Org. Chem.* **1988**, *53*, 918–920. (e) Denmark, S. E.; Choi, J. Y. *J. Am. Chem. Soc.* **1999**, *121*, 5821–5822. (f) Lee, H. M.; Nolan, S. P. *Org. Lett.* **2000**, *2*, 2053–2055. (g) Itami, K.; Nokami, T.; Ishimura, Y.; Mitsudo, K.; Kamei, T.; Yoshida, J. *J. Am. Chem. Soc.* **2001**, *123*, 11577–11585, Tin: (h) Littke, A. F.; Fu, G. C. *Angew. Chem., Int. Ed.* **1999**, *38*, 2411–2413. (i) Grasa, G. A.; Nolan, S. P. *Org. Lett.* **2001**, *3*, 119–122. (j) Mee, S. P. H.; Lee, V.; Baldwin, J. E. *Angew. Chem., Int. Ed.* **2004**, *43*, 1132–1136.
(25) (a) Korn, T. J.; Cahiez, G.; Knochel, P. *Synlett* **2003**, 1892–1894. (b) Ohmiya, H.; Yorimitsu, H.; Oshima, K. *Chem. Lett.* **2004**, *33*, 1240–1241. (c) Korn, T. J.; Knochel, P. *Angew. Chem., Int. Ed.* **2005**, *44*, 2947–2951. (d) Korn, T. J.; Schade, M. A.; Wirth, S.; Knochel, P. *Org. Lett.* **2006**, *8*, 725–728. (e) Korn, T. J.; Schade, M. A.; Cheemala, M. N.; Wirth, S.; Guevara, S. A.; Cahiez, G.; Knochel, P. *Synthesis* **2006**, 3547–3574.
(26) (a) Corriu, R. J. P.; Masse, J. P. *J. Chem. Soc. Chem. Commun.* **1972**, 144. (b) Tamao, K.; Sumitani, K.; Kumada, M. *J. Am. Chem. Soc.* **1972**, *94*, 4374–4376. (c) Tamao, K.; Sumitani, K.; Kiso, Y.; Zembayashi, M.; Fujioka, A.; Kodama, S.; Nakajima, I.; Minato, A.; Kumada, M. *Bull. Chem. Soc. Jpn.* **1976**, *49*, 1958–1969. (d) Böhm, V. P. W.; Weskamp, T.; Gstöttmayr, C. W. K.; Herrmann, W. A. *Angew. Chem., Int. Ed.* **2000**, *39*, 1602–1604. (e) Böhm, V. P. W.; Gstöttmayr, C. W. K.; Weskamp, T.; Herrmann, W. A. *Angew. Chem., Int. Ed.* **2001**, *40*, 3387–3389. (f) Dankwardt, J. W. *Angew. Chem., Int. Ed.* **2004**, *43*, 2428–2432. (g) Ackermann, L.; Born, R.; Spatz, J. H.; Meyer, D. *Angew. Chem., Int. Ed.* **2005**, *44*, 7216–7219. (h) Yoshikai, N.; Mashima, H.; Nakamura, E. *J. Am. Chem. Soc.* **2005**, *127*, 17978–17979. (i) Matsubara, K.; Ueno, K.; Shibata, Y. *Organometallics* **2006**, *25*, 3422–3427.
(27) (a) Quintin, J.; Franck, X.; Hocquemiller, R.; Figadére, B. *Tetrahedron Lett.* **2002**, *43*, 3547–3549. (b) Sapountzis, I.; Lin, W. W.; Kofink, C. C.; Despotopoulou, C.; Knochel, P. *Angew. Chem., Int. Ed.* **2005**, *44*, 1654–1658. (c) Kofink, C. C.; Blank, B.; Pagano, S.; Götz, N.; Knochel, P. *Chem. Commun.* **2007**, 1954–1956.
(28) (a) Norinder, J.; Matsumoto, A.; Yoshikai, N.; Nakamura, E. *J. Am. Chem. Soc.* **2008**, *130*, 5858–5859. (b) Yoshikai, N.; Matsumoto, A.; Norinder, J.; Nakamura, E. *Angew. Chem., Int. Ed.* **2009**, *48*, 2925–2928.

Table 1. Effect of Iron Salts and Additives on the Cross-Coupling of Chlorobenzene with *p*-TolMgBr

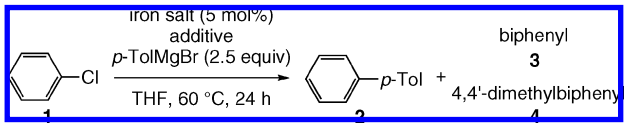

entry[a]	iron salt	additive (mol %)	% yields[b] 2	% yields[b] 3	RSM[c] 1	bitolyl[d] 4
1	**$FeF_3 \cdot 3H_2O$**	**SIPr·HCl (15)**	**98**	trace	0	4
2	$FeF_3 \cdot 3H_2O$	SIMes·HCl (15)	34	trace	64	5
3	$FeF_3 \cdot 3H_2O$	IPr·HCl (15)	25	trace	71	4
4	$FeF_3 \cdot 3H_2O$	SIPr·HBF_4 (15)	39	trace	48	6
5	$FeF_3 \cdot 3H_2O$	I-*t*-Bu·HCl (15)	51	trace	48	6
6	$FeF_3 \cdot 3H_2O$	SIPr·HCl (10)	93	trace	5	4
7	$FeF_3 \cdot 3H_2O$	SIPr·HCl (5)	61	trace	36	5
8	$FeF_3 \cdot 3H_2O$	none	6	trace	93	4
9	$FeF_3 \cdot 3H_2O$	PCy_3 (10)	5	0	87	4
10	$FeF_3 \cdot 3H_2O$	DPPE (10)	0	0	100	3
11	$FeF_3 \cdot 3H_2O$	DPPF (10)	1	0	99	4
12	$FeF_3 \cdot 3H_2O$	phenanthroline (5)	1	0	95	6
13	$FeF_3 \cdot 3H_2O$	TMEDA (2.5 equiv)	1	0	95	8
14	$FeF_2 \cdot 4H_2O$	SIPr·HCl (15)	96	trace	2	4
15	FeF_3	SIPr·HCl (15)	29	trace	69	2
16	FeF_2	SIPr·HCl (15)	18	trace	81	1
17[e]	FeF_3	H_2O (15), SIPr·HCl (15)	40	trace	57	1
18	$FeCl_3$	SIPr·HCl (15)	32	2	10	32
19	$Fe(acac)_3$	SIPr·HCl (15)	26	2	18	29
20	$FeCl_3$	none	17	2	17	33
21[f]	$FeCl_3$	KF (20), SIPr·HCl (15)	92	1	0	8

[a] Reactions were carried out on a 0.4−1.0 mmol scale. [b] The yield was determined by GC analysis using undecane as an internal standard. [c] Recovery of starting material. [d] Based on the amount of *p*-TolMgBr used. [e] Iron salt and additives were mixed in THF for 10 min at room temperature prior to the reaction. [f] $FeCl_3$ was treated with KF in MeOH/THF, which were then removed in vacuo.

Chart 1. Imidazolium and Imidazolinium Salts Examined as NHC Ligand Precursors

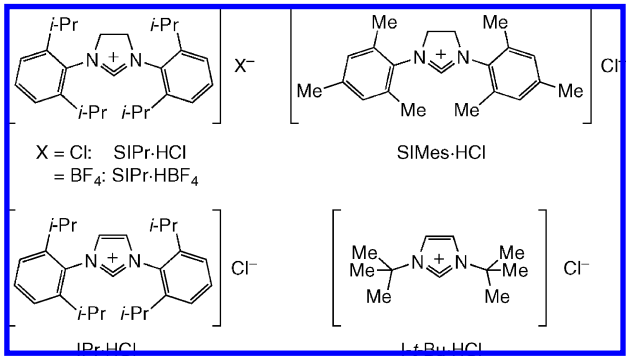

16). Note that the addition of 15 mol % of water into FeF_3 increased the product yield to a limited extent (entry 17). We assume that water or hydroxide can react with the solid surface of FeF_3 and make it partially soluble to promote the generation of catalytically active species to some extent.[29] In fact, a mixture of anhydrous FeF_3 and SIPr·HCl (1:2 ratio), finely ground under an inert atmosphere, showed the comparable reactivity with the combination of $FeF_3 \cdot 3H_2O$ and SIPr·HCl (data not shown). In the presence of $FeCl_3$ or $Fe(acac)_3$, homocoupling was predominant with or without SIPr·HCl (entries 18−20). Pretreatment of $FeCl_3$ with KF also generated a catalytically active species, which gave the unsymmetrical biaryl with the same efficiency of the catalyst prepared from the hydrates of iron fluorides (entry 21). This experiment indicates that the involvement of H_2O or metal hydroxide to the catalytic C−C bond-forming process is likely very minimal.

Cobalt- and Nickel Fluorides/NHC-Catalyzed Biaryl Cross-Coupling Reactions. We next focused on cobalt[30] and nickel[31] catalysts. Although various salts and complexes of these metals have been widely used as highly reactive metal catalysts for various C−C bond-forming reactions, the corresponding metal fluorides have only been minimally studied in the cross-coupling field.[32] We examined the reaction of chlorobenzene **1** with *p*-TolMgBr in the presence of catalytic amounts of cobalt and nickel fluorides with various NHCs and confirmed that high selectivity for the unsymmetrical biaryl can also be attained with these iron-group metal fluorides (Table 2).

The reaction with $CoF_2 \cdot 4H_2O$ (3 mol %) and IPr·HCl (6 mol %) gave **2** in a higher yield than **3** and **4** (95%, 3%, and 11% yields, respectively, entry 1), while the reaction with $CoCl_2 \cdot 6H_2O$ gave **2** with a considerable amount of **3** and **4** (68%, 11%, and 15% yields, respectively, entry 2). CoF_2 and CoF_3 showed lower catalytic activity that we attribute to their low solubility, similar to the anhydrous iron fluorides (entries 3 and 4). IPr·HCl emerged as the most effective NHC precursor rather than SIPr·HCl, as in entry 5. A similar "fluoride effect" was observed using nickel catalysts. The reaction with NiF_2 or $NiF_2 \cdot 4H_2O$ (1 mol %) and IPr·HCl (2 mol %) gave **2** selectively, but using $NiCl_2$ or $NiCl_2 \cdot 6H_2O$ resulted in less selectivity (entries 6−9). In the presence of a reduced amount of NiF_2 (0.5 mol %), the reaction was complete after 48 h, affording 98% yield of **2** (entry 10). In contrast to the iron catalyst, the counteranion of the NHC precursors did not affect the product yield (entry 11). Decreasing the steric bulkiness of the *N*-aryl substituent led to a decrease in product yield (entries 12 and 13). SIPr·HCl was slightly less effective than IPr·HCl (entry 14). It is noteworthy that addition of KF to $NiCl_2$ improved the cross-/homo-selectivity in the reaction of bromobenzene with *p*-TolMgBr (entries 15−17). From these results, we chose SIPr·HCl for iron fluoride and IPr·HCl for cobalt

(29) In $FeF_3 \cdot 3H_2O$ and $FeF_2 \cdot 4H_2O$, each iron atom is surrounded not only by fluorine atoms but also by water molecules in the form of a nearly regular octahedron. It can account for higher solubility of $FeF_3 \cdot 3H_2O$ and $FeF_2 \cdot 4H_2O$ than that of FeF_3 and FeF_2, in which an iron atom is surrounded by six fluorine atoms: (a) Hepworth, M. A.; Jack, K. H.; Peacock, R. D.; Westland, G. J. *Acta Crystallogr.* **1957**, *10*, 63–69. (b) Penfold, B. R.; Taylor, M. R. *Acta Crystallogr.* **1960**, *13*, 953–955. (c) Teufer, G. *Acta Crystallogr.* **1964**, *17*, 1480. (d) Jørgensen, J.-E.; Smith, R. I. *Acta Crystallogr.* **2006**, *B62*, 987–992.

(30) Recent reviews: (a) Shinokubo, H.; Oshima, K. *Eur. J. Org. Chem.* **2004**, 2081–2091. (b) Blekkan, E. A.; Borg, O.; Froeseth, V.; Holmen, A. *Catalysis* **2007**, *20*, 13–32. (c) Gosmini, C.; Bégouin, J.-M.; Moncomble, A. *Chem. Commun.* **2008**, 3221–3233. (d) Hess, W.; Treutwein, J.; Hilt, G. *Synthesis* **2008**, 3537–3562. (e) Jeganmohan, M.; Cheng, C.-H. *Chem. Eur. J.* **2008**, *14*, 10876–10886.

(31) Recent reviews: (a) Suginome, M.; Ito, Y. *J. Organomet. Chem.* **2003**, *680*, 43–50. (b) Montgomery, J. *Angew. Chem., Int. Ed.* **2004**, *43*, 3890–3908. (c) Netherton, M. R.; Fu, G. C. *Adv. Synth. Catal.* **2004**, *346*, 1525–1532. (d) Tamaru, Y., Ed.; *Modern Organonickel Chemistry*; Wiley-VCH: Weinheim, 2005. (e) Montgomery, J.; Sormunen, G. J. *Top. Curr. Chem.* **2007**, *279*, 1–23. (f) Kimura, M.; Tamaru, Y. *Top. Curr. Chem.* **2007**, *279*, 173–207. (g) Mori, M. *Eur. J. Org. Chem.* **2007**, 4981–4993. (h) Ng, S.-S.; Ho, C.-Y.; Schleicher, K. D.; Jamison, T. F. *Pure Appl. Chem.* **2008**, *80*, 929–939. (i) Nakao, Y.; Hiyama, T. *Pure Appl. Chem.* **2008**, *80*, 1097–1107. (j) Hirano, K.; Yorimitsu, H.; Oshima, K. *Chem. Commun.* **2008**, 3234–3241.

(32) Reviews for transition-metal fluoride: (a) Doherty, N. M.; Hoffmann, N. W. *Chem. Rev.* **1991**, *91*, 553–573. (b) Murphy, E. F.; Murugavel, R.; Roesky, H. W. *Chem. Rev.* **1997**, *97*, 3425–3468. (c) Mezzetti, A.; Becker, C. *Helv. Chem. Acta* **2002**, *85*, 2686–2703.

Table 2. Screening of Cobalt and Nickel Salts in the Presence of Various NHC Ligands

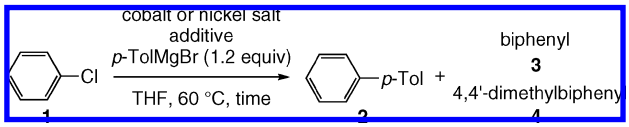

entry[a]	metal salt (mol %)	additive (mol %)	time (h)	% yields[b] 2	% yields[b] 3	RSM[c] 1	bitolyl[d] 4
1	**$CoF_2 \cdot 4H_2O$ (3)**	**IPr·HCl (6)**	48	**95**	3	0	11
2	$CoCl_2 \cdot 6H2O$ (3)	IPr·HCl (6)	48	68	11	2	15
3	CoF_2 (3)	IPr·HCl (6)	48	21	trace	79	2
4	CoF_3 (3)	IPr·HCl (6)	48	33	1	58	5
5	$CoF_2 \cdot 4H_2O$ (3)	SIPr·HCl (6)	48	39	trace	50	5
6	**NiF_2 (1)**	**IPr·HCl (2)**	24	**98**	trace	trace	3
7	$NiF_2 \cdot 4H_2O$ (1)	IPr·HCl (2)	24	96	trace	1	1
8	$NiCl_2$ (1)	IPr·HCl (2)	15	64	18	5	23
9	$NiCl_2 \cdot 6H_2O$ (1)	IPr·HCl (2)	15	60	18	11	22
10	**NiF_2 (0.5)**	**IPr·HCl (1)**	48	**98**	trace	0	2
11	**NiF_2 (0.5)**	**IPr·HBF_4 (1)**	48	**98**	trace	0	1
12	NiF_2 (0.5)	I-*t*-Bu·HCl (1)	48	95	trace	3	3
13	NiF_2 (0.5)	IMes·HCl (1)	48	7	trace	92	2
14	NiF_2 (0.5)	SIPr·HCl (1)	48	94	2	4	10
15[e]	$NiCl_2$ (1)	IPr·HCl (2)	1	83	14	0	20
16[e]	$NiCl_2$ (1)	KF (2), IPr·HCl (2)	1	95	3	0	5
17[e]	$NiCl_2$ (1)	KF (4), IPr·HCl (2)	1	96	2	0	4

[a] Reactions were carried out on a 1.0−3.0 mmol scale. [b] The yield was determined by GC analysis using undecane as an internal standard. [c] Recovery of starting material. [d] Based on the amount of *p*-TolMgBr used. [e] Bromobenzene was used instead of chlorobenzene.

and nickel fluorides as the standard NHC ligand in the ensuing investigations.

Biaryl Cross-Coupling Reactions in the Presence of Phosphine Lignads. Since the seminal work reported by Kumada and Tamao,[26b,c,33] phosphine ligands such as chelating 1,2-bis(diphenylphosphino)ethane (DPPE) and 1,3-bis(diphenylphosphino)propane (DPPP), have been known to be effective and widely used in the cross-coupling reactions with nickel as well as palladium catalysts. We therefore compared these orthodox diphosphine and monophosphine ligands with the NHC ligands in the nickel- or cobalt fluoride-catalyzed biaryl cross-coupling reactions (Table 3).

Cross-coupling reaction between bromobenzene and *p*-TolMgBr was catalyzed by NiF_2 in the absence of an auxiliary ligand to give a mixture of cross- and homocoupling products (**2**, **3**, and **4**) as in entry 1. Triphenylphosphine (PPh_3) did not accelerate cross-coupling but reduced the amounts of both homocoupling products **3** and **4** to some extent (entry 2). Addition of 4 equiv of PPh_3 to NiF_2 improved the cross-/homo-selectivity (entry 3). $NiCl_2$ catalyzed the coupling reaction with a slightly lower selectivity under the same conditions (entry 4). In sharp contrast to the earlier studies on the Kumada coupling, the chelating diphosphine ligands, DPPE, DPPP, and DPPB, prevented the cross-coupling reaction in the presence of NiF_2 (entries 5−7). These results can be explained by the "fluoride-effect," where the strong coordination of two fluoride ions and bisphosphine to the nickel center occupies four coordination sites, and therefore, one coordination site remains as a reactive site, which would be not suitable for the cross-coupling reaction (see the mechanistic studies below). Note that the representative nickel catalyst, $NiCl_2 \cdot$dppp, gave sufficient

(33) Kumada, M. *Pure. Appl. Chem.* **1980**, *52*, 669–679.

Table 3. Fluoride Effect on Ni- and Co-Catalyzed Biaryl Cross-Coupling in the Presence of Phosphine Ligands

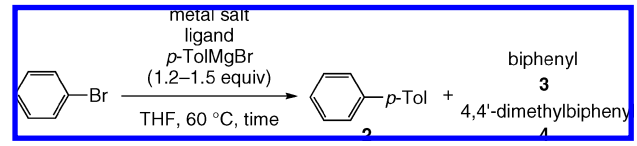

entry[a]	metal salt (mol %)	ligand (mol %)	time (h)	% yields[b] 2	% yields[b] 3	RSM [c]Ph−Br	bitolyl [d]4
1	NiF_2 (1)	none	22	59	32	0	40
2	NiF_2 (1)	PPh_3 (1)	16	57	15	0	25
3	NiF_2 (1)	PPh_3 (4)	16	93	6	0	14
4	$NiCl_2$ (1)	PPh_3 (4)	1	84	8	7	20
5	NiF_2 (1)	DPPE (1)	16	trace	0	99	3
6	NiF_2 (1)	DPPP (1)	16	trace	0	99	3
7	NiF_2 (1)	DPPB (1)	16	1	1	99	3
8	$NiCl_2 \cdot$dppp (1)	none	4	92	7	0	13
9	NiF_2 (0.5)	IPr·HCl (1)	3	99	trace	0	2
10	$CoF_2 \cdot H_2O$ (1)	none	16	12	trace	64	20
11	$CoF_2 \cdot 4H_2O$ (1)	DPPE (1)	16	1	0	93	4
12	$CoF_2 \cdot 4H_2O$ (0.5)	IPr·HCl (1)	3	99	0	0	7

[a] Reactions were carried out on a 1.0−3.0 mmol scale. [b] The yield was determined by GC analysis using undecane as an internal standard. [c] Recovery of starting material. [d] Based on the amount of *p*-TolMgBr used.

yield of **2** (92%), albeit with a considerable by-production of **3** and **4** (7% and 13% yields, respectively, entry 8). As in entry 9, excellent yield and selectivity were attained by using 0.5 mol % of NiF_2 and 1 mol % of IPr·HCl. Analogous to the nickel fluoride catalysis, DPPE prevented the coupling reaction with cobalt fluoride, while IPr dramatically accelerated the reaction (entries 10−12). In combination with the data for the iron fluoride catalysts (Table 1, entries 8−11), we conclude that the prevailing chelating diphosphines are ineffective ligands for the present metal fluoride-catalyzed cross-coupling reactions.

Preparation of Active Metal Catalyst by Pretreatment with Alkyl Grignard Reagents. Having confirmed the unique high selectivity of the cross-coupling catalysts consisting of an iron-group metal fluoride and an NHC, we sought to demonstrate the synthetic versatility and practicality of this novel biaryl cross-coupling reaction. The aforementioned procedure requires an excess amount of arylmagnesium bromide to achieve complete conversion of aryl halide. For example, the cross-coupling between chlorobenzene **1** and *p*-TolMgBr using a reduced amount of iron fluoride catalysts (3 mol % vs 5 mol %) and Grignard reagents (1.5 equiv vs 2.5 equiv) did not go to completion and gave the cross-coupling product in only 72% yield after 24 h at 60 °C (entry 1 in Table 4 vs entry 1 in Table 1). We assumed that insufficient basicity of the Grignard reagent toward deprotonation of NHC precursors and hydrates of iron or cobalt fluorides resulted in the slow conversion of substrate.[34] After screening various bases, MeMgBr and EtMgBr were found to be suitable for the activation of iron and cobalt composites (entries 2−8, Table 4). The treatment of $FeF_3 \cdot 3H_2O$ and SIPr·HCl with 18 mol % of MeMgBr to quench all protons derived from catalyst precursors enhanced the reaction rate to give **2** in 97% yield with 1% recovery of **1** (entry 2). Additional MeMgBr slightly enhanced the reaction rate (entry 3). With EtMgBr (18 mol %), the reaction completed to give 98% yield using 1.2 equiv of *p*-TolMgBr (entry 4). When 27 mol % of

(34) In situ generation of NHC ligand: Herrmann, W. A. *Angew. Chem., Int. Ed.* **2002**, *41*, 1290–1309, and references cited therein.

Table 4. Effect of MeMgBr and EtMgBr as an Activating Agent

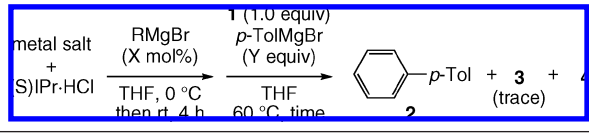

entry[a]	metal salt (mol %) (*S*) IPr·HCl (mol %)	R	X	Y	time (h)	% yield[b] **2**	RSM[c] **1**	bitolyl[d] **4**
1	$FeF_3 \cdot 3H_2O$ (3)	–	0	1.5	4	32	64	2
	SIPr·HCl (9)				24	72	25	3
2	$FeF_3 \cdot 3H_2O$ (3)	Me	18	1.2	4	52	45	2
	SIPr·HCl (9)				24	97	1	3
3	$FeF_3 \cdot 3H_2O$ (3)	Me	27	1.2	4	78	16	1
	SIPr·HCl (9)				24	97	trace	3
4	$FeF_3 \cdot 3H_2O$ (3)	Et	18	1.2	4	92	6	2
	SIPr·HCl (9)				12	**98**	0	3
5	$FeF_3 \cdot 3H_2O$ (3)	Et	27	1.2	4	89	9[e]	1
	SIPr·HCl (9)				24	96	0[e]	2
6	$CoF_2 \cdot 4H_2O$ (3)	–	0	1.5	4	11	84	4
	IPr·HCl (6)				24	56	42	7
7	$CoF_2 \cdot 4H_2O$ (3)	Me	18	1.2	4	68	32	4
	IPr·HCl (6)				24	93	4	4
8	$CoF_2 \cdot 4H_2O$ (3)	Et	18	1.2	4	55	42	3
	IPr·HCl (6)				24	**98**	2	3
9	NiF_2 (1)	–	0	1.2	4	65	33	1
	IPr·HCl (2)				24	**98**	1	1
10	NiF_2 (1)	Me	2	1.2	4	60	39	2
	IPr·HCl (2)				24	94	2	2

[a] Reactions were carried out on a 0.4–2.0 mmol scale. [b] The yield was determined by GC analysis using undecane as an internal standard. [c] Recovery of starting material. [d] Based on the amount of *p*-TolMgBr used. [e] Ethylbenzene was obtained in 3% yield.

EtMgBr was used for the generation of the active catalyst, ethylbenzene was obtained in 3% yield via cross-coupling of the residual EtMgBr and **1** (entry 5). Given the lower yield (2%) of the homocoupling product **4**, we assume that some of the excess EtMgBr is consumed by the partial reduction of the iron (III) to iron (II).[35] Similarly, pretreatment of $CoF_2 \cdot 4H_2O$ (3 mol %) and IPr·HCl (6 mol %) with 18 mol % of MeMgBr or EtMgBr afforded a considerable enhancement of the reaction rate (entries 6–8). In contrast, NiF_2 (1 mol %) did not require the treatment with the alkyl Grignard reagents, and almost complete conversion of **1** was observed either with or without pretreatment (entries 9 and 10). Hence, we assume that EtMgBr is basic enough to react with the water molecules of the metal fluoride hydrates in the liquid–solid state, assisting in their dissolution. In the following section, we display the scope and limitations of the present coupling reactions according to the procedures presented in entries 4, 8, and 9 respectively.

Selective Biaryl Cross-Coupling Reactions Catalyzed by Iron-Group Metal Fluorides/NHC: Scope and Limitations. With the optimal conditions in hand, we examined fluoro-, bromo-, and iodobenzenes as electrophiles to determine the scope of the leaving group in the present reactions, (Table 5). Reactions with *p*-TolMgBr (1.2 equiv) were conducted at 60 °C in the presence of $FeF_3 \cdot 3H_2O$ and SIPr·HCl (3 and 6 mol %, respectively), NiF_2 and IPr·HCl (0.5 and 1 mol %, respectively), or $CoF_2 \cdot 4H_2O$ and IPr·HCl (0.5 and 1 mol %, respectively).

(35) Although alkyl Grignard reagents possessing b-hydrogens are known to reduce some iron (III) and also iron (II) salts to zero or much lower oxidation states (see ref 15o and references cited therein), we are supposing the coordinating fluoride ion could hamper the full reduction of the iron salts in the light of the stoichiometric control experiments and theoretical studies described in the later part of the manuscript.

Table 5. Leaving Group Capabilities

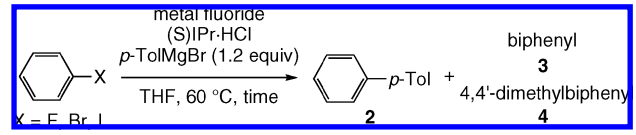

entry[a]	metal fluoride (mol %)	(*S*) IPr·HCl (mol %)	X	time (h)	% yields[b] **2**	% yields[b] **3**	RSM[c] Ph–X	bitolyl[d] **4**
1	$FeF_3 \cdot 3H_2O$ (3)	SIPr·HCl (9)	F	24	0	0	>99	trace
2	$FeF_3 \cdot 3H_2O$ (3)	SIPr·HCl (9)	Br	24	28	1	0	36
3	$CoF_2 \cdot 4H_2O$ (0.5)	IPr·HCl (1)	Br	3	99	trace	0	7
4	NiF_2 (0.5)	IPr·HCl (1)	Br	3	99	trace	0	2
5	NiF_2 (0.5)	IPr·HCl (0.5)	Br	3	98	2	0	4
6[e]	NiF_2 (0.5)	IPr·HCl (0.5)	Br	3	99	trace	0	2
7	NiF_2 (1.0)	none	Br	22	59	32	0	40
8	$NiCl_2$·dppp (1)	–	Br	4	92	7	0	13
9	$FeF_3 \cdot 3H_2O$ (3)	SIPr·HCl (9)	I	24	23	2	0	38
10	$CoF_2 \cdot 4H_2O$ (0.5)	IPr·HCl (1)	I	3	30	trace	10	44
11[f]	NiF_2 (0.5)	IPr·HCl (1)	I	1	92	1	0	11

[a] Reactions were carried out on a 1.0–3.0 mmol scale. [b] The yield was determined by GC analysis using undecane as an internal standard. [c] Recovery of starting material. [d] Based on the amount of *p*-TolMgBr used. [e] *p*-TolMgBr was added slowly over 3 h at 60 °C. [f] 3 mol % MeMgBr was added and stirred for 3 h at 60 °C before addition of iodobenzene and *p*-TolMgBr.

Fluorobenzene was fully inert under these conditions (entry 1). While the reaction of bromobenzene with the iron catalyst afforded predominantly the homocoupling product **4**, the reaction with cobalt or nickel catalyst gave **2** selectively (entries 2–4). As shown in entry 5, one equivalent of IPr·HCl for NiF_2 was ample for complete conversion, but not for complete selectivity. Interestingly, the selectivity was improved by the slow addition of *p*-TolMgBr to the reaction mixture (3 h at 60 °C, entry 6). The reaction without IPr·HCl was found to be slower and significantly less selective to give **2**, **3**, and **4** in 59%, 32%, and 40% yields, respectively (entry 7). Note that $NiCl_2$·dppp, a representative catalyst for the Kumada coupling, gave **2** with lower selectivity under the same conditions (entry 8). These results indicate that the NHC ligand (IPr or SIPr) not only accelerates the oxidative addition step due to its electron donation toward the metal center but also suppresses the homocoupling reaction. Bulky NHC ligands, such as IPr or SIPr, would prevent the formation of Ar_3M or rapid transmetalation (and the following nonselective coupling reaction) due to its steric hindrance. The reaction of iodobenzene showed the lowest selectivity in all cases (entries 9–11). Iodobenzene is a stronger oxidant than bromo- or chlorobenzene and can undergo oxidative addition to form a low-valent metal species that does not have an NHC ligand, which could subsequently form an Ar_3M species.

Regarding the substrate scope, the metal fluoride-catalyzed cross-coupling reaction can be widely applicable to a broad range of substrates (Table 6). We carried out coupling reactions using iron, cobalt, and nickel catalysts according to the procedure in entries 4, 8, and 9 in Table 4, respectively. Electron-rich 4-chloroanisole reacted smoothly with *p*-TolMgBr to give the desired product in 92%, 94%, and 88% yields, respectively (entry 1). Fluorine-substituted biaryls, the representative mesogen structure of liquid crystal molecules, can be synthesized with 1-chloro-4-fluorobenzene, 1-chloro-3,4-difluorobenzene, and 1-bromo-3,5-difluorobenzene in good to excellent yields with proper choice of a metal catalyst (entries

Table 6. Biaryl Cross-Coupling Catalyzed by Combinations of an Iron-Group Metal Fluoride and an NHC Ligand

entry[a]	Ar^1–X	Ar^2MgBr (equiv)	catalyst (mol%) conditions	% yield[b]
1	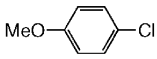	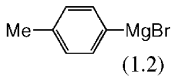 (1.2)	Fe cat. (3) 60 °C, 24 h	**92**
			Co cat. (3) 60 °C, 24 h	**94**[c]
			Ni cat. (3) 60 °C, 24 h	88[d]
2	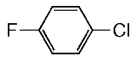	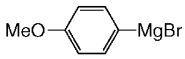 (1.2)	Fe cat. (3) 60 °C, 24 h	**91**
3	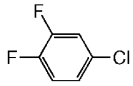	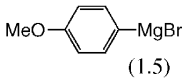 (1.5)	Fe cat. (5) 60 °C, 24 h 80 °C, 12 h	81
			Co cat. (5) 60 °C, 24 h	**97**
			Ni cat. (5) 60 °C, 24 h 80 °C, 12 h	46[c]
4	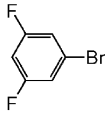	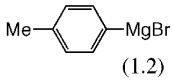 (1.2)	Fe cat. (5) 40 °C, 36 h	12[c]
			Co cat. (1) 40 °C, 36 h	20[c]
			Ni cat. (0.5) 40 °C, 18 h	**95**
5	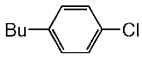	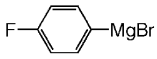 (1.5)	Fe cat. (4) 60 °C, 24 h	**87**
			Co cat. (4) 60 °C, 24 h	**86**[c]
			Ni cat. (4) 60 °C, 24 h	39[c]
6		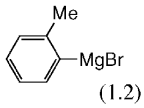 (1.2)	Fe cat. (3) 80 °C, 24 h	**90**
			Ni cat. (1) 60 °C, 36 h	**94**
7	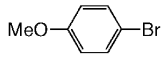	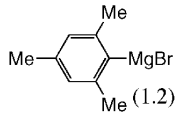 (1.2)	Co cat. (3) 80 °C, 24 h	84[c]
			Ni cat. (1) 80 °C, 12 h	**98**
8		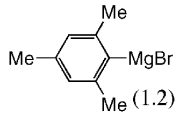 (1.2)	Fe cat. (3) 120 °C, 24 h[e]	**93**[c]
			Ni cat. (1) 120 °C, 4 h[e]	**96**
9	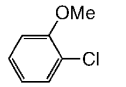	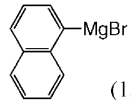 (1.2)	Fe cat. (5) 70 °C, 48 h	**92**
10	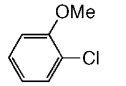	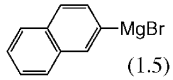 (1.5)	Fe cat. (3) 60 °C, 24 h	**96**
			Co cat. (3) 60 °C, 24 h	70[c]
			Ni cat. (3) 60 °C, 24 h	82[c]
11	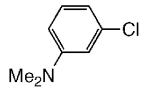	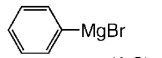 (1.2)	Fe cat. (3) 60 °C, 24 h	**94**
			Ni cat. (3) 60 °C, 24 h	41[c]
12	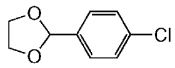	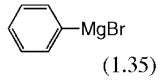 (1.35)	Fe cat. (3) 60 °C, 24 h 80 °C, 12 h	**88**
13	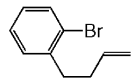	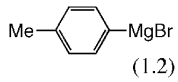 (1.2)	Fe cat. (5) 60 °C, 80 h	18[d]
			Co cat. (1) 60 °C, 4 h	82[d]
			Ni cat. (1) 60 °C, 18 h	**94**

[a] Reactions were carried out on a 1.0−3.0 mmol scale following the procedure in entries 4 (Fe cat.), 8 (Co cat.), and 9 (Ni cat.) in Table 4 unless otherwise noted. [b] Isolated yield. [c] The yield was determined by GC analysis using undecane as an internal standard. [d] The yield was determined by ^{1}H NMR analysis using bromoform or 1,1,2,2-tetrachloroethane as an internal standard. [e] The reaction was carried out in toluene.

2−4). In the case of 1-chloro-3,4-difluorobenzene, the cobalt catalyst gave a 97% yield of the desired product, but the nickel catalyst gave a much lower yield with considerable generation of defluorinated biaryl and tetraaryl compounds via C−F bond cleavage. On the other hand, 1-bromo-3,5-difluorobenzene selectively gave the desired product in the presence of the nickel catalyst owing to much higher reactivity of the C−Br bond than that of the C−F bond. The iron and cobalt catalysts gave 4,4′-dimethylbiphenyl as the major product via the homocoupling of *p*-TolMgBr (35% and 46%, respectively). Electron-deficient 4-fluorophenylmagnesium bromide gave the desired product in a good yield with the iron and cobalt catalysts, but a much lower yield with the nickel catalyst (entry 5). In the latter case, 40% of 1-butyl-4-chlorobenzene was recovered, and 10% of 4-butylbiphenyl was also obtained via C−F bond cleavage. While the reactions of *o*-tolyl- and mesitylmagnesium bromides were rather slow because of their steric hindrance, elevated reaction temperatures (80 and 120 °C) gave the corresponding products in good to excellent yields (entries 6−8). In these cases, the nickel catalyst showed higher catalytic activity than others. 1-Naphthylmagnesium bromide and 2-naphthylmagnesium bromide took part in the iron-catalyzed coupling reaction (92% and 96% yields, entries 9 and 10). The reactions of 2-naphthylmagnesium bromide with the cobalt and nickel catalysts were less selective, giving 70% and 82% yields of the desired product and 24% and 17% of 2,2′-binaphthyl, respectively. As shown in entry 11, the dimethylamino group seems to interfere with the nickel-catalyzed coupling reaction, but not the iron-catalyzed coupling reaction. Acetal functionality remained intact under the reaction conditions (entry 12). Whereas the reaction of 1-bromo-2-(but-3-enyl)benzene and *p*-TolMgBr with the nickel catalyst selectively gave the desired product, the reaction with the iron catalyst gave only 18% yield with 68% yield of 4,4′-dimethylbiphenyl via homocoupling reaction (entry 13).

Heteroaromatic nucleophiles, as well as electrophiles, took part in the selective biaryl cross-coupling reaction (Table 7). In the presence of the cobalt and nickel catalysts, 2-bromopyridine reacted with *p*-TolMgBr at 60 °C to give the desired product in

Table 7. Biaryl Cross-Couplings of Heteroaromatic Substrates

entry[a]	Ar^1–X	Ar^2MgBr (equiv)	catalyst (mol%) conditions	% yield[b]
1	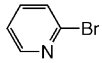	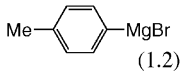 (1.2)	Fe cat. (2) 60 °C, 16 h	66[c]
			Co cat. (2) 60 °C, 16 h	**95**[c]
			Ni cat. (0.5) 60 °C, 16 h	**93**
2	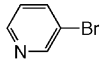	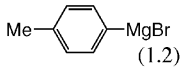 (1.2)	Fe cat. (2) 60 °C, 16 h	5[c]
			Co cat. (2) 60 °C, 16 h	4[c]
			Ni cat. (0.5) 60 °C, 16 h	**84**
3		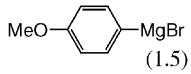 (1.5)	Fe cat. (4) 50 °C, 15 h	4[c]
			Co cat. (2) 50 °C, 15 h	**95**
			Ni cat. (1) 50 °C, 15 h	37[c]
4	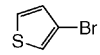	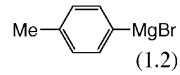 (1.2)	Fe cat. (2) 60 °C, 18 h	3[c]
			Co cat. (2) 60 °C, 18 h	**92**[c]
			Ni cat. (0.5) 60 °C, 18 h	**83**
5	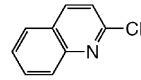	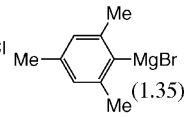 (1.35)	Fe cat. (3) 100 °C, 8 h[d]	**82**
6	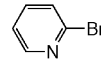	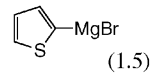 (1.5)	Fe cat. (6) 80 °C, 24 h	74
			Co cat. (6) 80 °C, 24 h	**99**[c]
			Ni cat. (3) 80 °C, 24 h	**99**[c]

[a] Reactions were carried out on a 1.0−3.0 mmol scale following the procedure in entries 4 (Fe cat.), 8 (Co cat.), or 9 (Ni cat.), Table 4 unless otherwise noted. [b] The isolated yield. [c] The yield was determined by GC analysis using undecane as an internal standard. [d] The reaction was carried out in toluene.

95% and 93% yields (entry 1). The reaction with the iron catalyst was less selective, yielding 66% of the desired product and 30% of 4,4′-dimethylbiphenyl via the homocoupling of *p*-TolMgBr. In these cases, 2-bromopyridine was not recovered. As shown in entry 2, the reaction between 3-bromopyridine and *p*-TolMgBr took place selectively with the nickel catalyst, but not with the iron or cobalt catalysts. The reaction with *p*-anisylmagnesium bromide took place selectively with the cobalt catalyst to give the desired product in 95% yield (entry 3). In the presence of the iron or nickel catalyst, the reaction did not go to completion, and 2-chlorothiophene was recovered (ca. 90% and 50%, respectively). 3-Bromothiophene gave the corresponding coupling product in good yields in the presence of the cobalt and nickel catalysts (entry 4). The reaction of 2-chloroquinoline with mesitylmagnesium bromide took place at 100 °C to give the desired product in 82% yield (entry 5). In the presence of the cobalt and nickel catalysts, the reaction of 2-bromopyridine with 2-thienylmagnesium bromide smoothly took place at 80 °C to give 2-thiophen-2-yl pyridine in 99% yield (entry 6).

Arenes bearing more than one leaving group can be selectively cross-coupled with a suitable catalyst (Tables 8 and 9). In the presence of the iron catalyst, the reaction of 4-chlorothioanisole **5** with *p*-TolMgBr took place via a selective C−Cl bond cleavage to give 4-methyl-4′-methylsulfanylbiphenyl **7** in 80% yield. The cobalt- and nickel-catalyzed reactions were less selective to afford **7** in 55% and 10% yields, respectively, with considerable amounts of side products (**6**, **8**, **2**, and **1**) via C−S bond cleavage.[36] Next, we carried out the reaction of 1-bromo-4-chlorobenzene with *p*-TolMgBr, as shown in Table 9. The reaction with the iron catalyst stopped after initial turnovers, with formation of a considerable amount of homocoupling product **4** and chlorobenzene **1**. This suggests that **9** served as an oxidant for

Table 8. Selective C−Cl Cleavage over C−S by Iron Catalyst

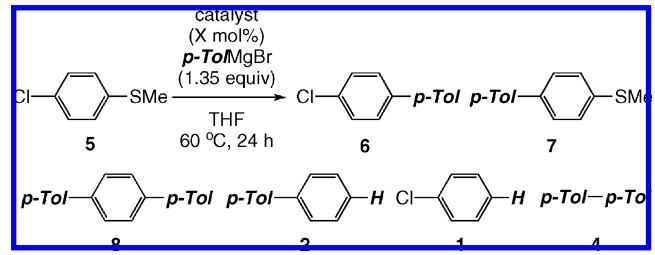

catalyst (X mol %)	% yields of product[a] 6	7	8	2	1	RSM[b] 5	bitolyl[c] 4
$FeF_3 \cdot 3H_2O$ (6), SIPr·HCl (18)	0	**80**	4	0	0	15	8
$CoF_2 \cdot 4H_2O$ (6), IPr·HCl (12)	2	55	6	0	0	29	7
NiF_2 (2), IPr·HCl (4)	2	10	13	6	17	30	10

[a] The yield was determined by GC analysis using undecane as an internal standard. [b] Recovery of starting material. [c] Based on the amount of *p*-TolMgBr used.

the homocoupling of *p*-TolMgBr to give 4-chlorophenylmagnesium bromide. The nickel catalyst turned out to be the best catalyst for the selective coupling to give a 4-chloro-4′-methylbiphenyl **6** in 96% yield.[37] In contrast, the cobalt catalyst gave a moderate yield and selectivity.

The present method is also useful for multiple arylation reactions of polychloroarenes. In the presence of the nickel catalyst prepared from nickel fluoride (6 mol %), IPr·HCl (12 mol %), and MeMgBr (24 mol %), the reaction between 1,2,4,5-tetrachlorobenzene **11** and phenylmagnesium bromide (PhMgBr) at 60−80 °C afforded 1,2,4,5-tetraphenylbenzene **12** in 71% yield and 1,2,4-triphenylbenzene in 20% yield (eq 1). Note that

(36) Tiecco, M.; Testaferri, L.; Tingoli, M.; Chianelli, D.; Wenkert, E. *Tetrahedron Lett.* **1982**, *23*, 4629–4632.

(37) (a) Ikoma, Y.; Taya, F.; Ozaki, E.-i.; Higuchi, S.; Naoi, Y.; Fuji-i, K. *Synthesis* **1990**, 147–148. (b) Littke, A. F.; Dai, C. Y.; Fu, G. C. *J. Am. Chem. Soc.* **2000**, *122*, 4020–4028.

Table 9. Selective C−Br Cleavage over C−Cl by Nickel Catalyst

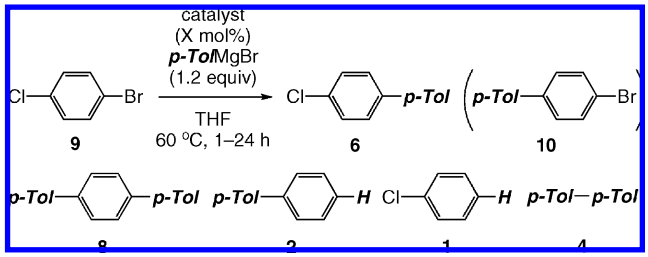

catalyst (X mol %)	% yields of product[a] 6	10	8	2	1	RSM[b] 9	bitolyl[c] 4
$FeF_3 \cdot 3H_2O$ (6), SIPr·HCl (18)	4	0	3	5	16	62	28
$CoF_2 \cdot 4H_2O$ (6), IPr·HCl (12)	78	0	3	2	11	0	13
NiF_2 (2), IPr·HCl (4)	**96**	0	2	0	0	0	3

[a] The yield was determined by GC analysis using undecane as an internal standard. [b] Recovery of starting material. [c] Based on the amount of *p*-TolMgBr used.

the reaction with 6 mol % of $NiCl_2 \cdot$dppp was sluggish (12% yield) under the same conditions.[38,39]

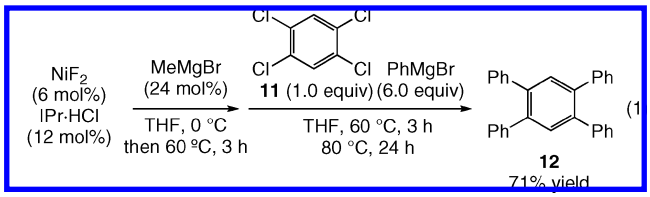

Mechanistic Considerations on the Catalytic "Fluoride Effect". To gain mechanistic insights into the origin of the high cross-/homo-selectivity of the metal fluoride catalysts, we conducted a series of control experiments and theoretical studies. The results of control experiments using a variety of metal salts, NHC ligand precursors (SIPr·HCl or IPr·HCl), *p*-TolMgBr are summarized in Scheme 3 and Table 10. The reactions were carried out in the absence of an aryl halide, which has been reported to accelerate the reductive elimination of neutral organonickel compounds,[40] and we observed a stark difference between the reactivities of the metal chloride and fluoride toward the Grignard reagent. As shown in Scheme 3, treatment of 0.1 mmol of $FeCl_2$ with *p*-TolMgBr (20 equiv) at 0 °C in the presence of SIPr·HCl (3.0 equiv) gave 0.096 mmol of 4,4′-dimethylbiphenyl **4** (96% yield based on the amount of $FeCl_2$). Similarly, treatment of $FeCl_3$ with *p*-TolMgBr under the same conditions gave 1.5 times as much of the stoichiometric amount of **4** as when $FeCl_2$ was treated with the Grignard reagent. These results clearly indicate that *p*-TolMgBr reduces the metal chlorides to give the corresponding metal (0) species and the biaryl product simultaneously, which corresponds to the initial activation step in the cross-coupling reaction. On the contrary, iron (II or III) fluorides did not afford **4** under the same conditions. Only a small amount of **4** was formed at 60 °C (with FeF_2 and FeF_3 in 6% and 11% yields, respectively), while the biaryl cross-coupling reaction took place smoothly at the same

(38) An improved yield (58%) has been achieved using 7.5 mol % of $Ni(acac)_2$ and a hydroxyphosphine. See ref 26h.

(39) Palladium-catalyzed tetraarylation of 1,2,4,5-tetrabromobenzene has been reported. (a) Berthiol, F.; Kondolff, I.; Doucet, H.; Santelli, M. *J. Organomet. Chem.* **2004**, *689*, 2786–2798. (b) Li, Z. H.; Wong, M. S.; Tao, Y. *Tetrahedron* **2005**, *61*, 5277–5285.

(40) Uchino, M.; Yamamoto, A.; Ikeda, S. *J. Organomet. Chem.* **1970**, *24*, C63−C64.

Scheme 3. Reaction of Iron Salts with *p*-TolMgBr in the Presence of SIPr·HCl

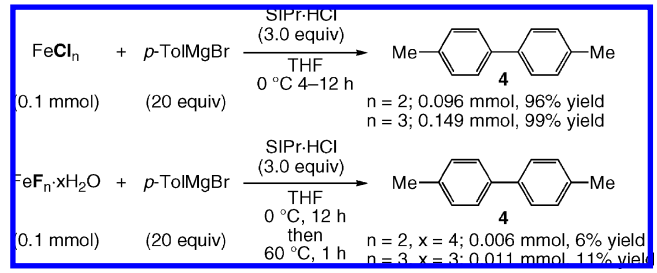

Table 10. Reaction of Cobalt and Nickel Salts with *p*-TolMgBr in the Presence of IPr·HCl

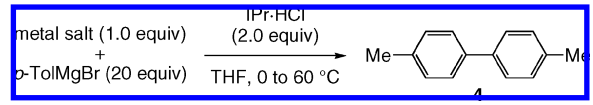

entry[a]	metal salt	conditions	bitolyl[b] 4
1	$CoCl_2 \cdot 6H_2O$	0 °C, 1 h	99
2	$NiCl_2$	0 °C, 1 h	98
3	$CoF_2 \cdot 4H_2O$	0 °C, 1 h	0
		60 °C, 1 h	8
4	NiF_2	0 °C, 1 h	0
		60 °C, 1 h	7
		60 °C, 4 h	11

[a] Reactions were carried out on a 0.1 mmol scale. [b] The yield was based on the amount of metal salts used and determined by GC analysis using undecane as an internal standard.

temperature in the presence of an aryl halide. Table 10 summarizes the results of similar control experiments for cobalt and nickel halides. Treatment of cobalt and nickel chlorides with *p*-TolMgBr resulted in the rapid homocoupling of the Grignard reagents (0 °C, 1 h) to give **4** in quantitative yield as in entries 1 and 2. On the other hand, the corresponding fluorides of these metals did not react with the Grignard reagent under the same conditions. Homocoupling product **4** was obtained in 8−11% yield even at 60 °C.

In light of the thermal instability of homoleptic tetraphenylferrate species, such as $[Ph_4Fe]Li_2$,[41] we considered that the formation of the homoleptic metalate complex via the transmetalation and addition of an arylmagnesium reagent is dominant in the reaction of the metal chlorides. On the other hand, the sharp contrast observed in the reactivities of metal fluorides (no significant biaryl formation) suggests that the fluoride counterion may interfere with the formation of the fully arylated metalate complex presumably due to its strong coordination of fluoride to the iron-group metal center and high electronegativity.

The results of the control experiments using the iron-group metal(II) fluorides/NHC ligands (SIPr or IPr), and chlorobenzene **1** are summarized in Scheme 4: chlorobenzene **1** was recovered in 95−99% without any formation of byproducts after 24 h at 60 °C. Notably, oxidative addition of the aryl halide to the divalent metal fluorides does not occur when a Grignard reagent is not added, even in the presence of NHC ligands (*not* the NHC precursors). These results show that the generation of reactive intermediates requires the reaction of corresponding metal fluoride with an arylmagnesium reagent.

(41) Fürstner et al. reported that a divalent tetraphenylferrate complex, $[Ph_4Fe]Li_2$, is prone to decompose thermally to give biphenyl in the presence or absence of an oxidant. See ref 15o.

Scheme 4. Reaction of Metal Fluorides with Chlorobenzene in the Presence of NHC Ligands

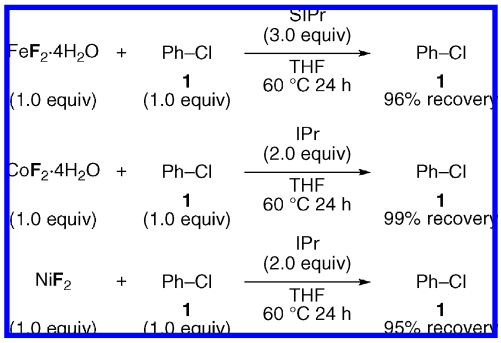

On the basis of these control experiments and the previously suggested reaction mechanisms involving the organometalate complexes of iron,[15o] cobalt,[42] and nickel[43] in cross-coupling reactions, we propose several plausible mechanisms shown in Figure 1. A metalate mechanism depicted in the left catalytic cycle starts with the formation of a heteroleptic metal (II)-ate complex **A** from a divalent metal fluoride and an arylmagnesium reagent (Ar^1MgX). The resulting heteroleptic metal (II)-ate complex **A** undergoes oxidative addition with an aryl halide to give an elusive higher-valent (formally IV oxidation state) species (**B**) carrying Ar^1 and Ar^2.[44] Subsequent reductive elimination to give the unsymmetrical biaryl (Ar^1-Ar^2) generates a metal (II) complex **C** bearing two fluorides and one halogen ligand derived from Ar^2X on the metal center. The reaction of **C** with Ar^1MgX regenerates the reactive intermediate **A**. A radical-type (II)−(III) mechanism has been reported for iron-catalyzed cross-coupling reaction of alkyl halides with arylmagnesium reagents.[45] The catalytic cycle depicted on the right side of Figure 1 shows a canonical "(0)−(II) mechanism", which consists of oxidative addition of an aryl halide to the metal (0) intermediate **D**, transmetalation between arylmetal halide **E** and Ar^1MgX, and reductive elimination of Ar^1-Ar^2 from diarylmetal(II) **F**.[46] We believe that the present reaction based on the metal fluoride catalyst does not take place via the popular (0)−(II) mechanism, but more likely via the higher-valent metalate mechanism, which is analogous to those of cuprate-mediated substitution reactions and catalytic cross-coupling reactions.[47] The final reductive elimination process in the "metalate mechanism" is presumed to be much faster than that of the "(0)−(II) mechanism" owing to instability of the high-valent intermediate **B**, thereby, prevailing over undesirable transmetalation or formation of -ate complexes carrying excess aryl groups (such as $Ar^1Ar^2{}_2M$, **G**).[48] The (0)−(II) and (II)−(IV) catalytic cycles have identical rate expressions and, thus, are kinetically indistinguishable as we assumed that the oxidative addition step is irreversible and the rate-limiting step.

In order to access the above-mentioned mechanistic considerations, we carried out computational studies to evaluate reaction pathways in the proposed mechanism starting from a metal (II)-ate complex. We chose a chemical model consisting of PhMgCl and PhCl, as the nucleophilic and electrophilic counterparts, and NiF_2 and I(Me) as the metal catalyst and the auxiliary ligand (eq 2). A DFT calculation method widely used for the mechanistic studies of the nickel catalyzed C−C bond formations were employed. The theoretical model is described as B3LYP/6-31G*.[49]

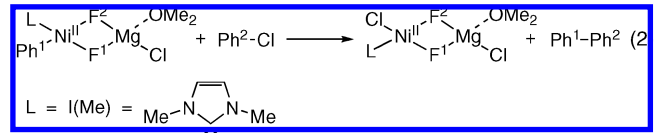

We could locate a single reaction pathway that connects the formation of a σ-complex, the oxidative addition of chlorobenzene (**Ph−Cl**), and the following reductive elimination of the biphenyl (**Ph−Ph**). Figure 2 displays the energy profile for the reaction pathway and Figure 3 summarizes the obtained structural information of the equilibrium and transition structures on the reaction coordinate. Nickelate complex (**$PhNiF_2$**) interacts with chlorobenzene to form σ-complex (**CP1**), which is 9.7 kcal/mol higher in energy (all electron energy, $\Delta\Delta E$) than the sum of **$PhNiF_2$** and **Ph−Cl**. The higher (uphill) energetics is likely due to the instability of the distorted square pyramidal structure of **CP1** (angles: $F^1-Ni-F^2 = 76.3°$, $Cl-Ni-F^2 = 75.0°$, $Cl-Ni-C^1 = 175.4°$ in Figure 3). The bond lengths indicate a weak electrostatic interaction between the nickel center and the lone electron pair of the chloride ligand (Ni−Cl = 2.690 Å, C^2-Cl = 1.773 Å, cf. C−Cl of Ph−Cl = 1.760 Å). The oxidative addition of **Ph−Cl** via **TS1** (C^2-Cl = 2.119 Å, $Ni-C^2$ = 2.107 Å, Ni−Cl = 2.313 Å) requires a reasonable activation energy ($\Delta E^{\ddagger} = +18.3$ kcal/mol) to form an octahedral Ni(IV) intermediate, **CP2** ($Ni-C^2$ = 1.945 Å, Ni−Cl = 2.352 Å). This transformation is endothermic ($\Delta\Delta E = +6.2$ kcal/mol), mirroring the elusive nature of a tetravalent organonickel species. The reductive elimination of **Ph−Ph** from **CP2** successively takes place via **TS2** (C^1-C^2 = 2.215 Å, $Ni-C^1$ = 1.983 Å, $Ni-C^2$ = 1.978 Å) with a very small activation energy ($\Delta E^{\ddagger} =$

(42) Wakabayashi, K.; Yorimitsu, H.; Oshima, K. *J. Am. Chem. Soc.* **2001**, *123*, 5374–5375.

(43) (a) Terao, J.; Watanabe, H.; Ikumi, A.; Kuniyasu, H.; Kambe, N. *J. Am. Chem. Soc.* **2002**, *124*, 4222–4223. (b) Terao, J.; Todo, H.; Watanabe, H.; Ikumi, A.; Kambe, N. *Angew. Chem., Int. Ed.* **2004**, *43*, 6180–6182.

(44) Organometal (IV) compounds: (a) Bower, B. K.; Tennent, H. G. *J. Am. Chem. Soc.* **1972**, *94*, 2512–2514. (b) Byrne, E. K.; Theopold, K. H. *J. Am. Chem. Soc.* **1989**, *111*, 3887–3896. (c) Dimitrov, V.; Linden, A. *Angew. Chem., Int. Ed.* **2003**, *42*, 2631–2633. (d) Carnes, M.; Buccella, D.; Chen, J. Y.-C.; Ramirez, A. P.; Turro, N. J.; Nuckolls, C.; Steigerwald, M. *Angew. Chem., Int. Ed.* **2009**, *48*, 290–294.

(45) Noda, D.; Sunada, Y.; Hatakeyama, T.; Nakamura, M.; Nagashima, H. *J. Am. Chem. Soc.* **2009**, *131*, 6078–6079.

(46) Although the canonical mechanism has been widely accepted for Pd-catalyzed cross-coupling reactions, several alternatives have been proposed for the cross-coupling reactions based on the first-row transition metal catalysts including Fe, Co, and Ni. See refs 14f, 15o, 26c, 42, and 43.

(47) (a) Nakamura, E.; Mori, S.; Morokuma, K. *J. Am. Chem. Soc.* **1998**, *120*, 8273–8274. (b) Mori, S.; Nakamura, E.; Morokuma, K. *J. Am. Chem. Soc.* **2000**, *122*, 7294–7307.

(48) $[Ar_4Fe^{III}][Li(THF)_3]$: (a) Alonso, P. J.; Arauzo, A. B.; Forniés, J.; Garcia-Monforte, M. A.; Martin, A.; Martinez, J. I.; Menjón, B.; Rillo, C.; Sáiz-Garitaonandia, J. J. *Angew. Chem., Int. Ed.* **2006**, *45*, 6707–6711$[Me_4Fe^{II}]$ $[Li(OEt_2)]_2$: (b) Fürstner, A.; Krause, H.; Lehmann, C. W. *Angew. Chem., Int. Ed.* **2006**, *45*, 440–444. Fe−F complex: (c) Vela, J.; Smith, J. M.; Yu, Y.; Ketterer, N. A.; Flaschenriem, C. J.; Lachicotte, R. J.; Holland, P. L. *J. Am. Chem. Soc.* **2005**, *127*, 7857–7870.

(49) The DFT calculations were performed using the B3LYP hybrid functional and the 6-31G* basis set. All stationary points were optimized without any symmetry assumptions, and characterized all by normal coordinate analysis at the same level of the geometry optimization. Details are described in the Supporting Information. Theoretical studies using DFT method on (0)−(II) mechanism for nickel-catalyzed cross-coupling and related reactions: Reinhold, M.; McGrady, J. E.; Perutz, R. N. *J. Am. Chem. Soc.* **2004**, *126*, 5268–5267, and references cited therein. See also a recent paper: Yoshikai, N.; Matsuda, H.; Nakamura, E. *J. Am. Chem. Soc.* **2008**, *130*, 15258–15259.

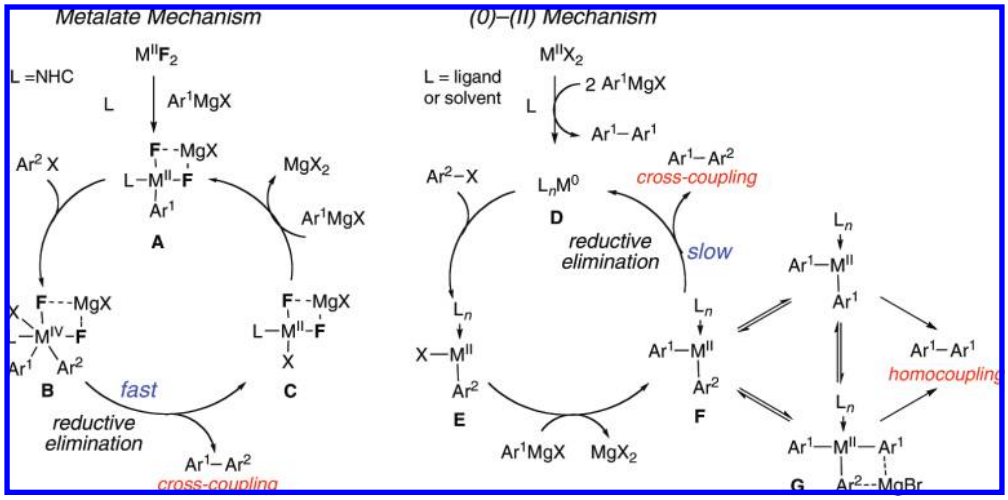

Figure 1. Plausible mechanism: metal−fluoride-ate complex as a reactive intermediate.

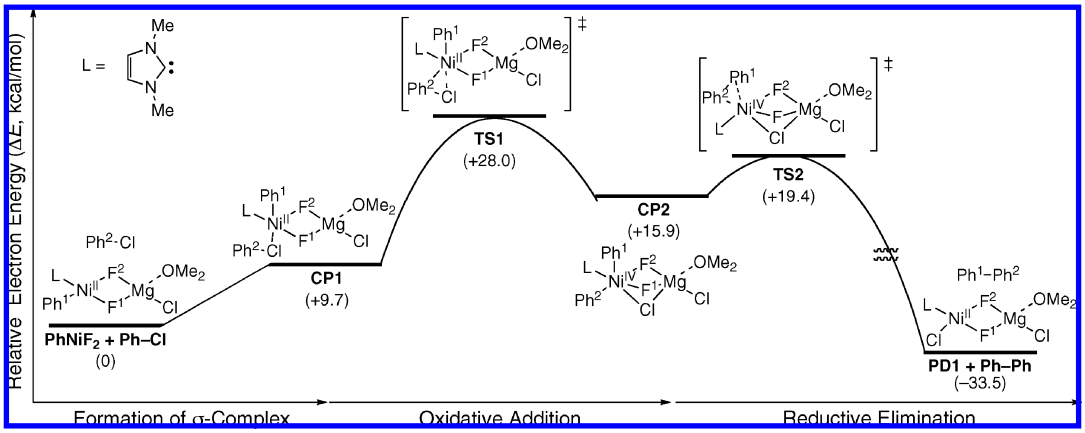

Figure 2. Energy profiles for the metalate mechanism based on the DFT calculation (B3LYP/6-31G*). Relative electron energies based on **PhNiF$_2$** plus **Ph−Cl** (ΔE, kcal/mol) are shown in parentheses.

+3.5 kcal/mol) to form a square-planar Ni(II) complex **PD1** with a stabilization energy of 49.4 kcal/mol. The calculated low activation barrier of the reductive elimination and the large exothermicity suggests that the reductive elimination pathway should be more favorable than an alternative transmetalation pathway of **CP2** with arylmagnesium reagents (see below). In light of the low activation barrier, one may expect that the tetravalent nickel intermediate would not be an equilibrium structure (a stationary point) when the NHC ligand carries sterically demanding aryl groups on the nitrogen atoms as in the real system.

We next examined the reaction of metal fluorides and arylmagnesium reagents using a chemical model consisting of a phenylmagnesium reagent, an NHC, and either nickel salts of NiF_2 or $NiCl_2$. This system corresponds to the control experiments described in Scheme 3 and Table 10. We adopted I(Me)NiX_2 (X = Cl or F) as the models of the catalyst precursors and examined the reaction with phenylmagnesium chloride solvated with two molecules of dimethyl ether (PhMgCl·2Me_2O) at the same level of theory (eq 3).

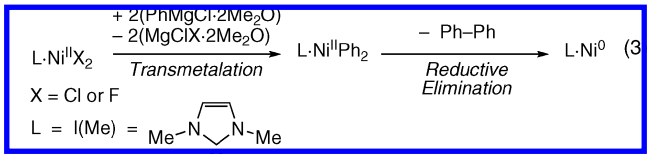

In each case of I(Me)$NiCl_2$ and I(Me)NiF_2 (denoted as **NiCl$_2$** and **NiF$_2$**, respectively), a single reaction pathway was obtained for transmetalation process with PhMgCl·2Me_2O (Path-A and Path-B, respectively) to form I(Me)$NiPh_2$ (denoted as **NiPh$_2$**). The energy profiles for Path-A and Path-B are shown in black and blue colors, respectively, in Figure 4. Shown as Path-C is the subsequent reaction pathway from the common intermediate, **NiPh$_2$** via a reductive elimination to give the biphenyl (**Ph−Ph**) and I(Me)Ni(0)-biphenyl η^4 complex (denoted as **Ni^0**).[50]

The starting NHC/nickel chloride complex **NiCl$_2$** and PhMgCl·2Me_2O formed a nickelate complex (**PhNiCl$_2$**) after releasing one molecule of a solvent, Me_2O, in a highly exothermic manner ($\Delta\Delta E = -42.7$ kcal/mol). The formation of the neutral phenylnickel species I(Me)PhNiCl (denoted as **PhNiCl**), upon the dissociation of $MgCl_2$·2Me_2O, was found to be 10.0 kcal/mol greater in energy.[51] The second molecule of PhMgCl·2Me_2O and **PhNiCl** formed the nickelate intermediate carrying two phenyl groups (denoted as **Ph$_2$NiCl**) in the same manner as the preceding formation of **PhNiCl$_2$**. This process is also exothermic ($\Delta\Delta E = -28.7$ kcal/mol). Diphenylnickel coordinated by the NHC ligand, (denoted **Ph$_2$Ni**) formed upon the dissociation of $MgCl_2$·2Me_2O in an endother-

(50) Molecular structures and all electron energies of the stationary points are described in the Supporting Information.

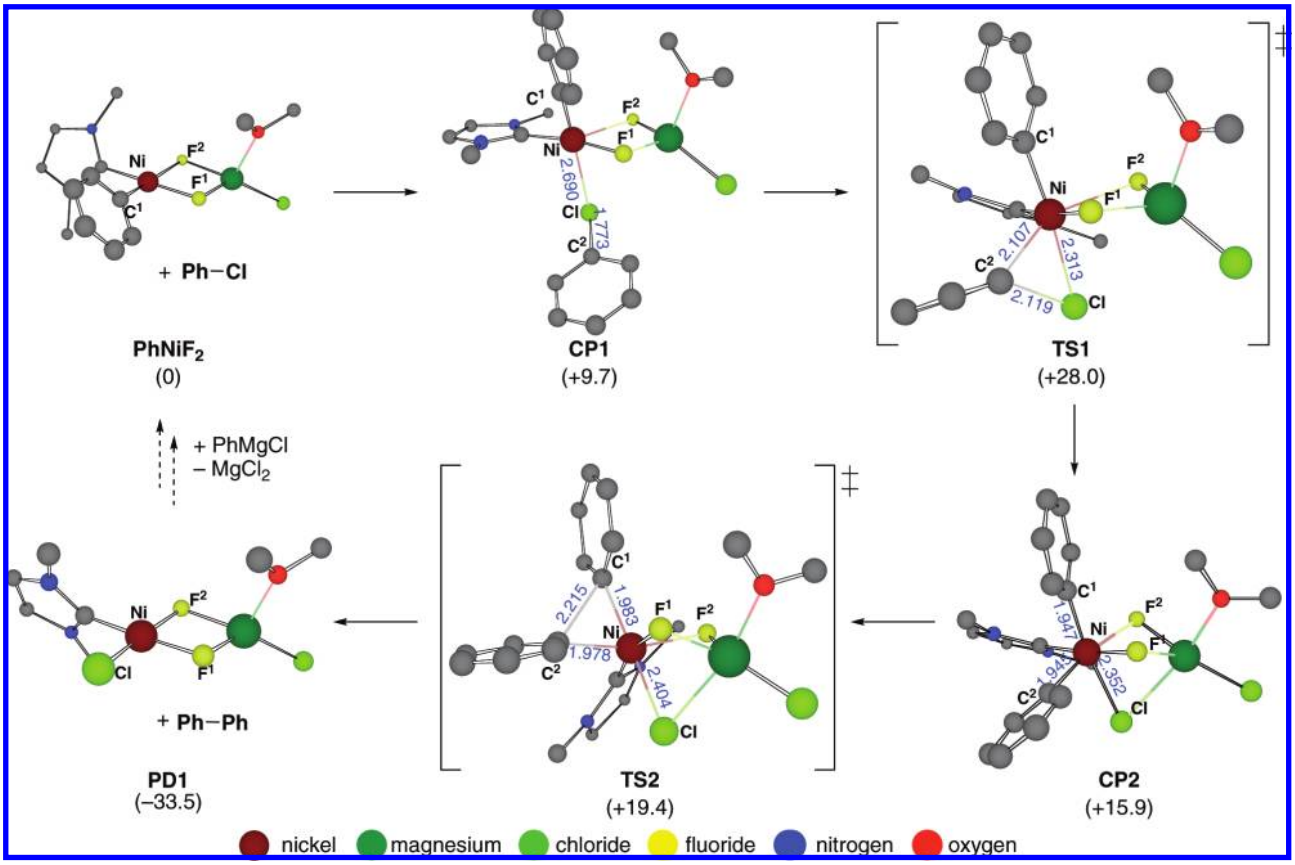

Figure 3. Reaction pathway for nickel fluoride-catalyzed cross-coupling based on the DFT calculation (B3LYP/6-31G*). Relative electron energies based on **PhNiF$_2$** plus **Ph−Cl** (ΔE, kcal/mol) are shown in parentheses. Bond lengths are given in Å. Hydrogen atoms are omitted for clarity.

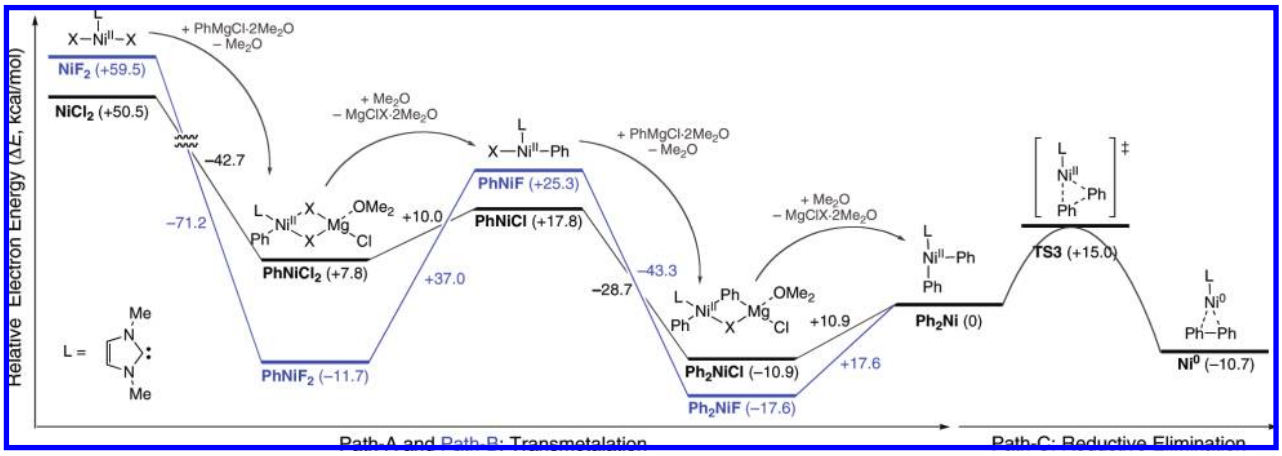

Figure 4. Energy profiles for the transmetalation and reductive elimination processes based on the DFT calculation (B3LYP/6-31G*). Relative electron energies based on **Ph$_2$Ni** (ΔE, kcal/mol) are shown in parentheses (Path-A, X = Cl: black; Path-B, X = F: blue; Path-C: black).

mic manner ($\Delta\Delta E = +10.9$ kcal/mol). The diphenylnickel species underwent reductive elimination to afford a biphenyl complex of the nickel (0) species **Ni**^{0} via a three-centered transition structure **TS3** with a reasonable activation barrier and exothermicity ($\Delta E^{\ddagger} = +15.0$ kcal/mol and $\Delta\Delta E = -10.7$ kcal/mol, respectively). The whole process starting from **NiCl$_2$** to **Ni**^{0} is exothermic ($\Delta\Delta E = -61.2$ kcal/mol) and the transformation from the initial nickelate complex **PhNiCl$_2$** into **Ni**^{0} is also found to be exothermic ($\Delta\Delta E = -18.5$ kcal/mol). Taking the whole reaction pathway into consideration, the DFT study suggests that the reduction of NiCl$_2$ with phenyl Grignard reagent should be facile in the presence of an NHC ligand, which agrees well with the experimental results described above.

The DFT calculations for the **NiF$_2$** system provided us with a similar sequence of transformations from the starting nickel fluoride into the zero-valent nickel species **Ni**^{0}, but its energy profile was notably different from the one obtained for the **NiCl$_2$** system (Path-A vs Path-B). Transformation from **NiF$_2$** into **Ph$_2$Ni** as in Path-B thus consists of four steps: (1) formation of the monophenyl nickelate complex **PhNiF$_2$** ($\Delta\Delta E = -71.2$ kcal/

(51) Other geometrical isomers are less stable than **PhNiX$_2$**. Details are described in the Supporting Information.

mol); (2) formation of a divalent phenyl nickel halide **PhNiF** upon the dissociation of $MgClF\cdot 2Me_2O$ ($\Delta\Delta E = +37.0$ kcal/mol); (3) formation of the diphenylnickelate complex **Ph_2NiF** ($\Delta\Delta E = -43.3$ kcal/mol); (4) formation of diphenylnickel species **Ph_2Ni** upon the dissociation of $MgClF\cdot 2Me_2O$ ($\Delta\Delta E = +17.6$ kcal/mol). After the formation of **Ph_2Ni**, each reaction pathway of **$NiCl_2$** and **NiF_2** merged into Path-C, resulting in the formation of **Ph−Ph** and **Ni^0** from **Ph_2Ni**. Although the overall process from **NiF_2** to **Ni^0** (Path-B and Path-C) is exothermic in total ($\Delta\Delta E = -70.2$ kcal/mol), energy minima of Path-B are at the stages of the organonickelate intermediates, **$PhNiF_2$** and **Ph_2NiF** ($\Delta\Delta E = -1.0$ and -6.9 kcal/mol, respectively). The most significant difference between Path-A and Path-B is the highly endothermic nature of the formation of the phenylnickel halide intermediates **PhNiF** from the nickelates **$PhNiF_2$** ($\Delta\Delta E = +37.0$ kcal/mol vs $+10.0$ kcal/mol for the formation of **PhNiCl** from **$PhNiCl_2$**). Cleavage of a strong Ni−F bond is energetically unfavorable and is presumably the origin of the large endothermicity. The large electron negativity of fluorine may account for the stabilization of the fluorinated nickelate complex and also contribute in part to the enhancement of the uphill energy difference. It is noteworthy that the activation barrier of the reaction of **$PhNiF_2$**and **Ph−Cl** is much lower ($\Delta E^{\ddagger} = +28.0$ kcal/mol as in Figure 2) than the endothermicity of the **PhNiF** formation ($\Delta\Delta E = +37.0$ kcal/mol). The results of the DFT calculations show that **$PhNiF_2$** is a reactive intermediate, which undergoes oxidative addition with an aryl halide substrate, and hence, a prime candidate of catalytically active species in the NiF_2−NHC-catalyzed selective biaryl cross-coupling.

We carried out the same DFT calculations adopting similar chemical models for the iron and cobalt fluorides−NHC-catalyzed biaryl coupling reactions. Because the difficulty of the treatment of multiple spin-state systems of these metals has been well-documented using the DFT method (a divalent iron can take $S = 0$, 1, and 2 spin states, and a divalent cobalt can take $S = 1/2$ and 3/2 spin states),[52] we carefully conducted computational studies on the critical early steps of the above-presented metalate mechanism of these metals. We thus compared the energies associated with the oxidative addition of chlorobenzene to the heteroleptic metalate complexes (**Ph-MF_2**, M = Fe or Co as shown in Figures 5 and 6, respectively) and the transmetalation from the metalates. As shown in Figure 5, we could locate the reaction coordinates of the quintet state ($S = 2$) and the triplet state ($S = 1$), but failed to obtain that of the singlet state ($S = 0$) for the iron catalyst. The oxidative addition of **Ph−Cl** to the ferrate complex in the quintet state, **$PhFeF_2$_q**, took place via **TS4_q** with a reasonable activation barrier ($\Delta E^{\ddagger} = +29.5$ kcal/mol) to give the tetravalent intermediate **CP3_q**. The activation energy is almost comparable to the endothermicity associated with the formation of the divalent phenyliron fluoride intermediate **PhFeF_q** by the

(52) Because the B3LYP functional have been known to overestimate the stability of high spin states, we examined several functionals including the one without HF exchange term (BP91) and the other with modified admixture of HF term (B3LYP*) to obtain the virtually same results. Further computational study on the present catalytic cross-coupling reactions waits for the development of multiconfigurational treatment such as CASSCF calculation using realistic chemical models, and of course, it has been so far impractical. Zein, S.; Borshch, S. A.; Fleurat-Lessard, P.; Casida, M. E.; Chermette, H. *J. Chem. Phys.* **2007**, *126*, 014105. For B3LYP* and the coefficient of exact exchange admixture in DFT calculation affects relative energies of states of different multiplicity; see: Reiher, M.; Salomon, O.; Hess, B. A. *Theor. Chem. Acc.* **2001**, *107*, 48−55.

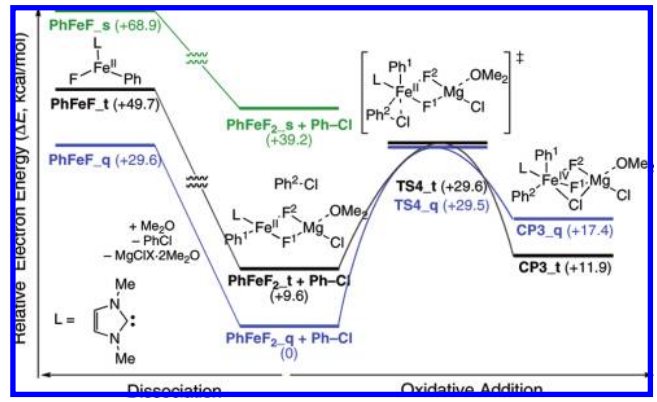

Figure 5. Energy profiles for the oxidative-addition and transmetalation processes based (B3LYP/6-31G*). Relative electron energies based on **$PhFeF_2$_q** plus **Ph−Cl** (ΔE, kcal/mol) are shown in parentheses (singlet state, $S = 0$: green; triplet state, $S = 1$: black; quintet state, $S = 2$: blue).

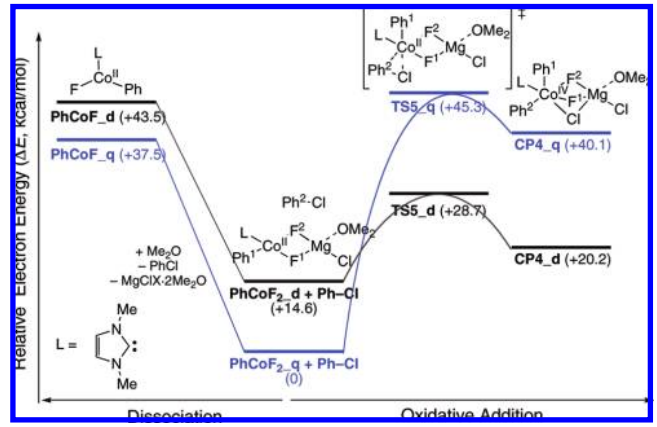

Figure 6. Energy profiles for the oxidative-addition and transmetalation processes (B3LYP/6-31G*). Relative electron energies based on **$PhCoF_2$_q** plus **Ph−Cl** (ΔE, kcal/mol) are shown in parentheses (doublet state, $S = 1/2$: black; quartet state, $S = 3/2$: blue).

dissociation of $MgClF\cdot 2Me_2O$ ($\Delta\Delta E = +29.6$ kcal/mol). In the reaction coordinate of the triplet state (shown in black line in Figure 5), it was found that the tetravalent intermediate **CP3_t** is slightly more stable than the one in the quintet state (**CP3_q**, $\Delta\Delta E_{t\text{-}q} = -5.5$ kcal/mol), whereas the other stationary points (**PhFeF_t**, **$PhFeF_2$_t**, and **TS4_t**) are more unstable than those in the quintet state ($\Delta\Delta E_{t\text{-}q} = +20.1$, $+9.6$, and $+0.1$ kcal/mol, respectively). We could locate only two stationary points **PhFeF_s** and **$PhFeF_2$_s** for the singlet state and confirmed the relative energy of these structures were much less stable than the corresponding structures in the triplet and quintet states.[53] From these results, it is supposed that the most stable **$PhFeF_2$_q** should be a reactive intermediate for the oxidative addition and the cross-coupling reaction should proceed in the quintet state to form the elusive iron (IV) intermediates tentatively, which may be prone to undergo a rapid reductive elimination to give the cross-coupling product (Ph^1−Ph^2).

We could locate reaction coordinates of the quartet state ($S = 3/2$) and the doublet state ($S = 1/2$) for the cobalt catalyst to notice that the energy profiles are more complicated. As shown in Figure 6, the potential energy surfaces of the quartet state and the doublet state cross over during

(53) No reaction pathway for oxidative addition process was obtained in singlet state.

the oxidative-addition process (the blue lines and the black lines, respectively). The cobaltate complex in the quartet state, **PhCoF$_2$_q**, is found to be more stable than the one in the doublet state, **PhCoF$_2$_d** ($\Delta\Delta E_{q\text{-}d} = -14.6$ kcal/mol). On the other hand, at the transition structure of the oxidative addition, the quartet state **TS5_q** is much less stable than the doublet state **TS5_d** ($\Delta\Delta E_{q\text{-}d} = +16.6$ kcal/mol). Analogously, at the tetravalent cobaltate intermediate, the quartet state **CP4_q** is much less stable than the doublet state **CP4_d** ($\Delta\Delta E_{q\text{-}d} = +19.9$ kcal/mol). These results indicate that, during the oxidative addition process, a crossover of reaction pathways between the quartet and doublet states may take place with the C−Cl bond cleavage occurring via **TS5_d** and leading the formation of **CP4_d** in the doublet state. The energy difference between **PhCoF$_2$_q** and **TS5_d** ($\Delta\Delta E = +28.7$ kcal/mol) is substantially smaller than the endothermicity of the formation of divalent phenylcobaltale fluoride intermediate **PhCoF_q** by dissociation of MgClF·2Me$_2$O ($\Delta\Delta E = +37.5$ kcal/mol). This energy profile suggests that the initial transmetalation of cobalt fluoride precatalyst is sluggish and the cobaltate complex **PhCoF$_2$_q** can be a reactive intermediate for the cobalt fluoride-catalyzed biaryl coupling reaction.

On the basis of the results of the control experiments and the theoretical studies, we conclude that strong coordination of the fluoride ion to the metal center suppresses the initial transmetalation and following reduction processes and a resulting heteroleptic metalate (II) complex such as **PhMF$_2$** can catalyze a biaryl cross-coupling reaction. A low activation barrier for the reductive elimination in the present metalate mechanism can account for the characteristically high cross-/homo-selectivity.

Conclusion

We developed a selective and practical biaryl cross-coupling reaction catalyzed by iron-group metal catalysts based on the synergistic modulation by the fluoride counterion and an NHC ligand. Experimental control reactions and theoretical calculations suggest that the catalytic "fluoride effect" underlies the observed high selectivity of cross-coupling over homocoupling in the reaction. Each of the iron-group metal catalysts possesses a characteristic catalytic reactivity profile; the appropriate choice of a metal fluoride−NHC ligand combination allows for the efficient coupling of a wide range of aryl nucleophile and electrophiles in excellent yield and high selectivity. First, the iron catalyst can achieve highly selective coupling reactions using various aryl chlorides. Second, the cobalt catalyst is particularly effective in heteroaromatic couplings. And third, the nickel catalyst shows high catalytic activity and a broad substrate scope when aryl bromides and sterically hindered substrates are employed. The present biaryl coupling features several synthetic advantages: (1) The catalytic method can achieve high-yielding unsymmetrical biaryl synthesis with an excellent cross-coupling selectivity. (2) The simple and scalable procedures of this coupling method are suitable for large-scale production. (3) This catalyst system is free of both palladium and phosphine. As for the origin of the catalytic "fluoride effect", a noncanonical mechanism is proposed, in which strong coordination of the fluoride ion to the divalent metal center suppresses the reduction of the metal via the conventional transmetalation reduction elimination process, and promotes the formation of a high-valent heteroleptic metalate complex. The resulting high-valent heteroleptic metalate complex catalyzes the desired biaryl cross-coupling with high selectivity over the undesired homocoupling. We believe that the concept of the synergistic effect of a fluoride ion and an auxiliary ligand will further advance the development of cross-coupling technologies, as well as relevant carbon−carbon bond-forming reactions, which are currently under investigation in this laboratory.

Experimental Section

Synthesis of 4-Methylbiphenyl (2): A Representative Procedure for the Iron-Catalyzed Reaction Shown in Tables 2, 4, and 6−9. A THF solution of ethylmagnesium bromide (5.00 mL, 1.08 M, 5.40 mmol) was added to FeF$_3$·3H$_2$O (0.150 g, 0.90 mmol) and 1,3-bis(2,6-diisopropylphenyl)imidazolinium hydrochloride (1.15 g, 2.70 mmol) at 0 °C. THF (1.0 mL) was added to rinse the vessel. After stirring at room temperature for 5 h, chlorobenzene (3.38 g, 30.0 mmol) and a THF solution of *p*-tolylmagnesium bromide (38.7 mL, 1.02 M, 36.0 mmol) was added at 0 °C. The reaction was carried out at 60 °C for 24 h. After cooling to ambient temperature, aqueous sodium potassium tartrate (saturated, 60.0 mL) was added. The aqueous layer was extracted five times with hexane. The combined organic extracts were filtered with a pad of Florisil. GC analysis was carried out (98% yield) using undecane as an internal standard. After the solvent was removed *in vacuo*, the crude product was purified by chromatography on silica gel (pentane) to obtain the title compound (4.97 g, 98% yield, > 98% pure on GC analysis) as a white solid.

Synthesis of 3,4-Difluoro-4′-methoxybiphenyl: A Representative Procedure for the Cobalt-Catalyzed Reaction Shown in Tables 3−9. A THF solution of ethylmagnesium bromide (0.55 mL, 1.08 M, 0.60 mmol) was added to CoF$_2$·4H$_2$O (17.0 mg, 0.10 mmol) and 1,3-bis(2,6-diisopropylphenyl)imidazolium hydrochloride (85.4 mg, 0.20 mmol), and THF (1.5 mL) at 0 °C. THF (0.5 mL) was added to rinse the vessel. After stirring at room temperature for 4 h, 4-chloro-1,2-difluorobenzene (0.297 g, 2.0 mmol) and a THF solution of 4-methoxyphenylmagnesium bromide (3.4 mL, 0.88 M, 3.0 mmol) was added at 0 °C. The reaction was carried out at 60 °C for 12 h. After cooling to ambient temperature, aqueous ammonium chloride (saturated, 2.0 mL) was added. The aqueous layer was extracted five times with Et$_2$O. The combined organic extracts were filtered with a pad of Florisil. After the solvent was removed *in vacuo*, the crude product was purified by chromatography on silica gel (0%, 5% toluene in hexane) to obtain the title compound (0.428 g, 97% yield, > 98% pure on GC analysis) as a white solid.

Synthesis of 3,5-Difluoro-4′-methylbiphenyl: A Representative Procedure for the Nickel-Catalyzed Reaction Shown in Tables 3−9. A THF solution of *p*-tolylmagnesium bromide (2.12 mL, 1.13 M, 2.4 mmol) was added to NiF$_2$ (0.97 mg, 0.010 mmol) and 1,3-bis(2,6-diisopropylphenyl)imidazolium hydrochloride (8.52 mg, 0.020 mmol), and 1-bromo-3,5-difluorobenzene (0.386 g, 2.0 mmol) at 0 °C. After stirring at room temperature for 0.5 h, the reaction was carried out at 40 °C for 18 h. After cooling to ambient temperature, aqueous ammonium chloride (saturated, 2.0 mL) was added. The aqueous layer was extracted five times with Et$_2$O. The combined organic extracts were filtered with a pad of Florisil. After the solvent was removed *in vacuo*, the crude product was purified by chromatography on silica gel (pentane) to obtain the title compound (0.388 g, 95% yield, > 98% pure on GC analysis).

Acknowledgment. We thank Japan Society for the Promotion of Science (JSPS) and the Ministry of Education, Culture, Sports, Science and Technology of Japan (MEXT) for financial supports; Grants-in-Aid for Scientific Research on Priority Areas "Synergistic Effects for Creation of Functional Molecules" (M.N., 18064006) and "Chemistry of Concerto Catalysis" (T.H., 20037033), and

Grant-in-Aids for Young Scientists from JSPS (S, M.N., 2075003; B, T.H., 2175098). Financial supports from the Uehara Memorial Foundation, Tosoh Finechem and Tosoh Corporations are gratefully acknowledged. This work has been supported in part by Global COE Program "International Center for Integrated Research and Advanced Education in Materials Science" and the Joint Project of Chemical Synthesis Core Research Institution from MEXT. We thank Dr. J. Hong for helpful discussion on the reaction mechanism and proofreading. We also thank Prof. H. Nagashima and Dr. Y. Sunada for valuable discussion. We are also thankful for helpful comments from reviewers and thorough proofreading by Dr. H. Seike.

Supporting Information Available: Experimental procedure and characterization data. This material is available free of charge via the Internet at http://pubs.acs.org.

JA9039289